

# The human chorion contains definitive hematopoietic stem cells from the fifteenth week of gestation

Marcus O. Muench<sup>1,2,\*</sup>, Mirhan Kapidzic<sup>3,4,\*</sup>, Matthew Gormley<sup>3,4</sup>, Alan G. Gutierrez<sup>3,4</sup>, Kathryn L. Ponder<sup>3,5</sup>, Marina E. Fomin<sup>1</sup>, Ashley I. Beyer<sup>1</sup>, Haley Stolp<sup>3,4</sup>, Zhongxia Qi<sup>6</sup>, Susan J. Fisher<sup>3,4</sup> and Alicia Bárcena<sup>3,4,†</sup>

## ABSTRACT

We examined the contribution of the fetal membranes, amnion and chorion, to human embryonic and fetal hematopoiesis. A population of cells displaying a hematopoietic progenitor phenotype (CD34<sup>++</sup> CD45<sup>low</sup>) of fetal origin was present in the chorion at all gestational ages, associated with stromal cells or near blood vessels, but was absent in the amnion. Prior to 15 weeks of gestation, these cells lacked hematopoietic *in vivo* engraftment potential. Differences in the chemokine receptor and  $\beta$ 1 integrin expression profiles of progenitors between the first and second trimesters suggest that these cells had gestationally regulated responses to homing signals and/or adhesion mechanisms that influenced their ability to colonize the stem cell niche. Definitive hematopoietic stem cells, capable of multilineage and long-term reconstitution when transplanted in immunodeficient mice, were present in the chorion from 15-24 weeks gestation, but were absent at term. The second trimester cells also engrafted secondary recipients in serial transplantation experiments. Thus, the human chorion contains functionally mature hematopoietic stem cells at mid-gestation.

**KEY WORDS:** Human hematopoietic stem cells, Chorion, Extraembryonic development, Hematopoietic development

## INTRODUCTION

Mammalian development entails asynchronous growth of the embryo/fetus and extraembryonic structures – principally, the placenta and membranes. The placenta, which develops in advance of the embryo/fetus to support its growth, was shown to be a hematopoietic organ in mice (Gekas et al., 2005; Ottersbach and Dzierzak, 2005) and humans (Barcena et al., 2009, 2011; Robin et al., 2009; Serikov et al., 2009). The placenta is composed of highly vascularized tree-like chorionic villi that sprout from the chorionic plate (CP) (Fig. 1A; Fig. S1A). The villous surface is covered by trophoblasts. During most of the first trimester, the chorion is also covered with villi, which regress into a bilayer of

cytotrophoblasts (CTBs) and stroma (Fig. 1B) to form the smooth chorion (SC) that surrounds the embryo/fetus, as the amniotic cavity enlarges (Benirschke et al., 2006). We reasoned that the common developmental origin of the placenta and the chorion (Hamilton and Boyd, 1960) might entail the simultaneous existence of cells with hematopoietic potential at both sites.

The anatomy of the fetal membranes is depicted in Fig. 1. The amnion, the inner layer, is the most proximal membrane to the embryo/fetus (Fig. 1A,B) and includes an epithelial monolayer. Beneath lies an avascular stromal layer (Luckett, 1975). The SC, the outer layer that lies adjacent to the decidual cells that line the uterus (Fig. 1A,B), comprises multiple layers of CTBs and a stroma that fuses with the amnion stroma in the mature fetal membrane (Bourne, 1962; Cross, 1998). The amniotic epithelium and CTBs are ectodermal derivatives; their stromata arise from the extraembryonic mesoderm. Initially, the chorion and amnion are physically separated and, as the pregnancy progresses, the amnion is positioned closer to the chorion and the adjacent stromal layers fully fuse at ~17-20 weeks of gestation (Ilancheran et al., 2009), forming the mature structure of the amnion-chorion (Fig. 1B; Fig. S1D).

The mouse chorion contains myeloid and definitive erythroid progenitors prior to chorio-allantoic fusion and before establishment of the fetal circulation within the placenta, suggesting the *in situ* generation of hematopoietic progenitors (Zeigler et al., 2006). Previously, we reported the presence of a population expressing high levels of CD34 and low levels of CD45 (CD34<sup>++</sup> CD45<sup>low</sup> cells) in whole human fetal membranes, but their niche and, more importantly, their functional status as hematopoietic precursors have not been established (Barcena et al., 2011). This population also resides in the chorionic villi of the placenta and contains hematopoietic stem cells (HSCs) (Barcena et al., 2011). Here, we asked whether the comparable region of the human chorion (Fig. 1B, dark blue) contains HSCs throughout gestation.

## RESULTS

### Hematopoietic progenitors in the extraembryonic compartment are restricted to the chorion and chorionic villi

To determine the exact location of phenotypically defined hematopoietic precursors observed in the amniochorion (Barcena et al., 2011) we isolated cells from the amnion, the chorion and, as a control, the chorionic villi from the same placentas across gestation and analyzed CD34 and CD45 (PTPRC) expression. The anatomical regions analyzed are depicted in Fig. S1. The 40 weeks of human pregnancy are often divided into trimesters: first (0-13 weeks), second (14-27 weeks) and third (28-40 weeks) trimester. The chorion samples contained both the SC and the CP, which was denuded of villi by manual dissection (Fig. S1A,B), and in those samples of amniochorion the amnion was separated from the chorion (Fig. S1C,E). The three tissues analyzed from first trimester samples were not subjected to any further processing after

<sup>1</sup>Blood Systems Research Institute, San Francisco, CA 94118, USA. <sup>2</sup>Department of Laboratory Medicine, University of California, San Francisco, CA 94143, USA. <sup>3</sup>The Ely and Edythe Broad Center of Regeneration Medicine and Stem Cell Research, University of California, San Francisco, CA 94143, USA. <sup>4</sup>Center of Reproductive Sciences, Department of Obstetrics, Gynecology & Reproductive Sciences, University of California, San Francisco, CA 94143, USA. <sup>5</sup>Department of Pediatrics, University of California, San Francisco, CA 94143, USA. <sup>6</sup>Department of Laboratory Medicine, Clinical Cytogenetics Laboratory, University of California, San Francisco, CA 94107, USA.

\*These authors contributed equally to this work

†Author for correspondence (Alicia.Barcelona@ucsf.edu)

ORCID: M.O.M., 0000-0001-8946-6605; M.G., 0000-0003-2042-1534; A.G.G., 0000-0002-8567-9598; M.E.F., 0000-0002-1573-8126; A.I.B., 0000-0002-9306-3515; H.S., 0000-0003-1635-894X; A.B., 0000-0003-3463-0628

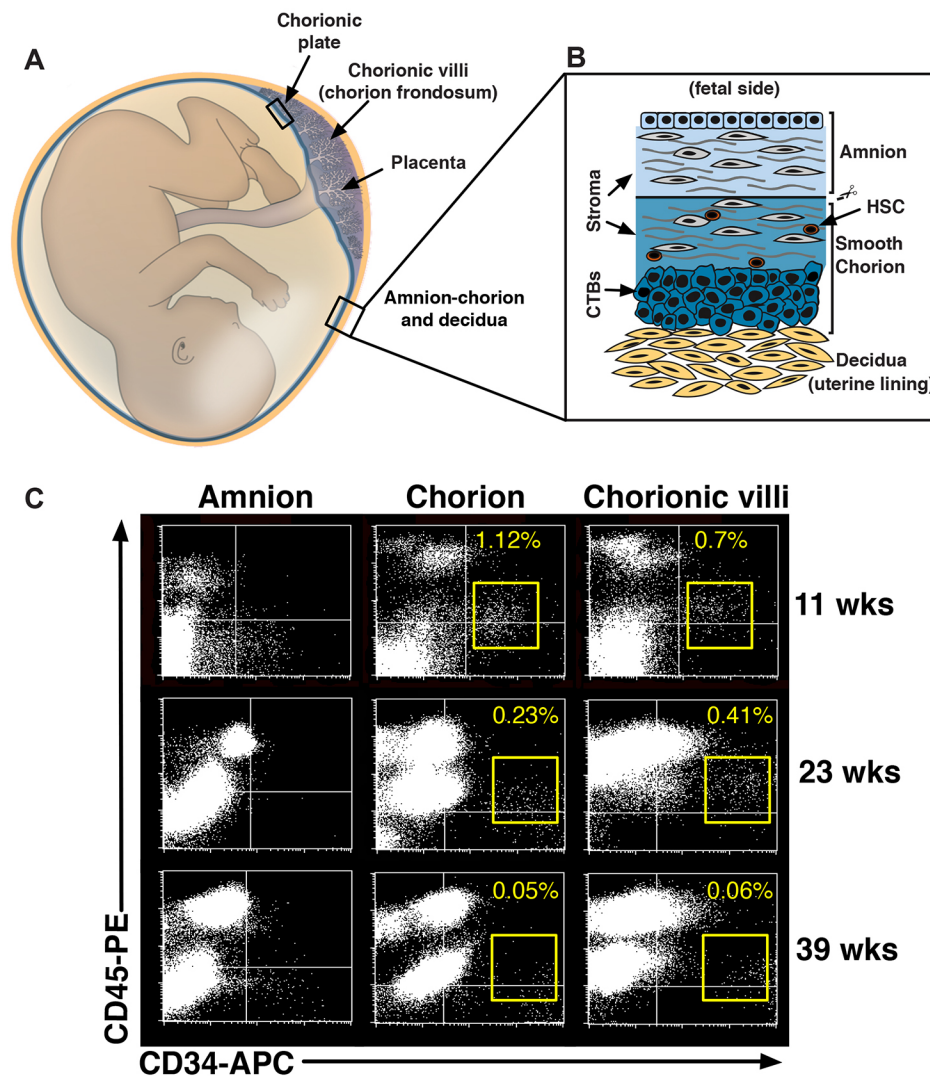


**Fig. 1. The human chorion contains HSCs.** (A) Anatomy of the embryonic and extraembryonic compartments at mid-gestation. The placenta contains chorionic villi that protrude from the chorionic plate (CP). The amnion-chorion is a bilayer (blue). The placenta and chorion are in direct contact with the decidua (yellow). (B) Basic histology of the amnion-smooth chorion (SC) at mid-gestation. The amnion (light blue) is composed of amniocytes (the monolayer at the top), which line the amniotic cavity, and an underlying stroma (gray cells). The SC, which shares the stroma (gray cells), contains multiple layers of cytotrophoblasts (CTBs; dark blue). The SC interfaces with the decidua. HSCs reside within the SC stroma. (C) Cell suspensions of freshly isolated amnion, chorion and chorionic villi were analyzed by FACS for CD34 and CD45 expression.  $2 \times 10^5$  viable cells were acquired and quadrants were set using isotype-matched controls. Yellow gates encompass the CD34<sup>++</sup> CD45<sup>low</sup> cells.  $n=6$  (one first trimester, three second trimester and two term). PE, phycoerythrin; APC, allophycocyanin.

the enzymatic digestion of the tissues as described (Barcena et al., 2009), whereas second and third trimester tissues were processed further to obtain the light-density fraction. Fig. 1C shows the absence of cells co-expressing CD34 and CD45 in the amnion. By contrast, hematopoietic progenitors (CD34<sup>++</sup> CD45<sup>low</sup> cells) were readily detected in the chorion and the chorionic villi at all gestational ages. CD34<sup>-</sup> CD45<sup>+</sup> mature cells were observed in all samples and their frequency increased during gestation (Fig. 1C). Most of these cells are Hofbauer cells, i.e. CD14<sup>+</sup> macrophages, which represent the most abundant mature hematopoietic cells in extraembryonic tissues (Barcena et al., 2009).

#### Immunolocalization of chorionic CD34<sup>+</sup> CD45<sup>low</sup> cells throughout gestation

To identify the hematopoietic niche in the chorion, we localized CD34<sup>+</sup> CD45<sup>+</sup> cells using immunofluorescence and confocal microscopy (Fig. 2). The sensitivity of immunofluorescence techniques does not allow high and low levels of CD34 expression to be distinguished, as is achieved by FACS. Therefore, we searched for cells coexpressing CD34 and CD45. Immunolocalization detected a similarly low frequency of chorionic hematopoietic progenitors as that observed by FACS analyses (Fig. 1C). These cells resided primarily within the mesenchymal compartment (Fig. 2A). During early gestation, when villi are

forming, clusters of CD34<sup>+</sup> CD45<sup>+</sup> cells were observed next to vimentin<sup>+</sup> cells (Fig. 2B). Regardless of age, these cells were frequently found in close contact with vimentin<sup>+</sup> mesenchymal cells in the CP (Fig. 2C,D). CD34<sup>+</sup> CD45<sup>+</sup> cells were also found in a predominantly perivascular location in the SC (Fig. 2E,F), near vessels containing CD34<sup>+</sup> CD45<sup>-</sup> endothelial cells. In addition, the number of individual and clusters of CD34<sup>+</sup> CD45<sup>+</sup> cells significantly increased from first to second trimester. In conclusion, CD34<sup>+</sup> CD45<sup>+</sup> cells were frequently found associated with vimentin<sup>+</sup> stromal cells in first trimester chorion, as well as in second trimester CP, and were primarily positioned near or within the vasculature in second trimester SC.

#### The frequency and number of CD34<sup>++</sup> CD45<sup>low</sup> cells vary across gestation

Hematopoietic progenitors were quantified from 51 chorion samples of different gestational ages. We defined a gate that contained the population of CD34<sup>++</sup> CD45<sup>low</sup> cells (Fig. 3A). Primitive hematopoietic progenitors and HSCs are known to display low levels of CD45 on their cell surface and to increase CD45 expression as they differentiate (Mayani et al., 1993). We found chorionic CD34<sup>++</sup> CD45<sup>low</sup> cells at low frequency throughout gestation (0.01-1.9%,  $n=51$ ). The density of CD34<sup>++</sup> CD45<sup>low</sup> cells, measured as the mean number of cells/g tissue, was highest at



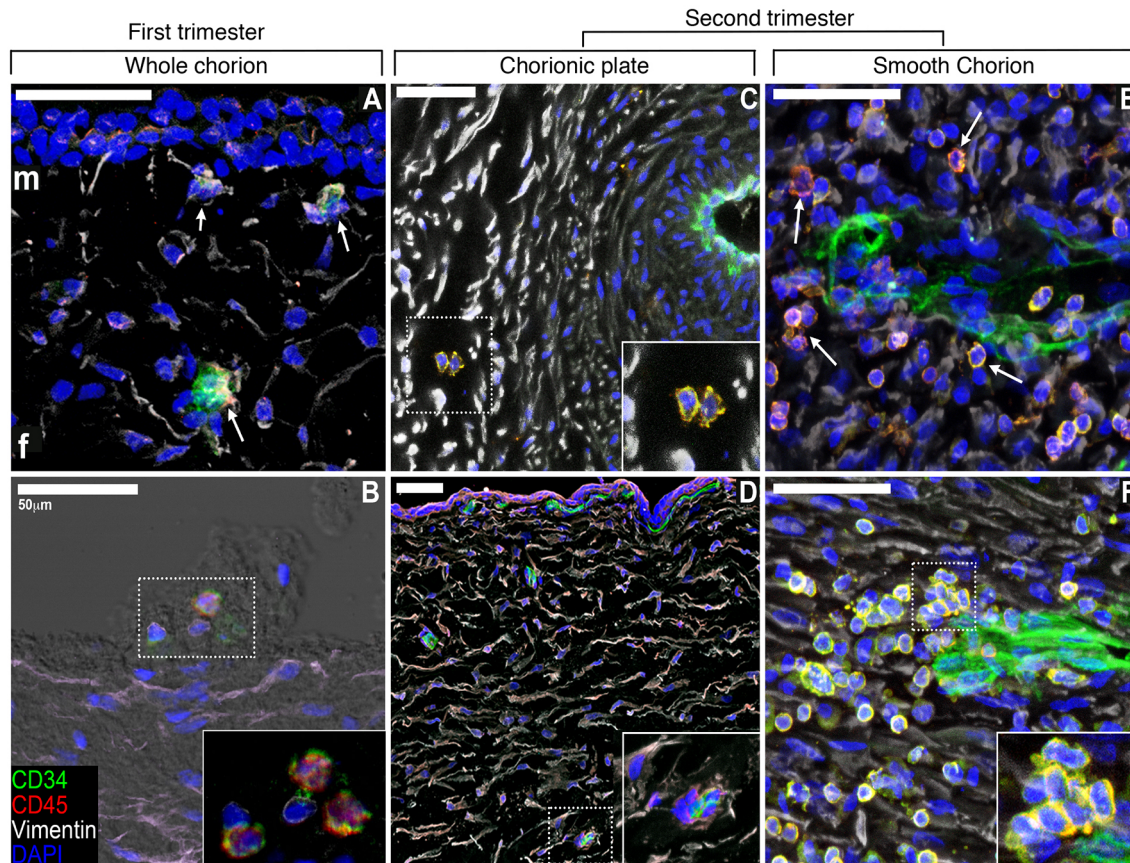


**Fig. 2. Immunolocalization analyses reveal the position of CD34<sup>++</sup> CD45<sup>low</sup> cells in first and second trimester chorion.** Tissue sections of human chorion were stained for CD34 (green), CD45 (red) and vimentin (white) and visualized by confocal microscopy. The panels are oriented showing fetal side (f) down and maternal side (m) up. Boxed regions (dotted lines) are magnified in insets. Cells that co-expressed CD34 and CD45 were found, either individually or as clusters, in proximity to vimentin<sup>+</sup> stromal cells (A-D). CD34<sup>+</sup> CD45<sup>+</sup> cells were also detected near blood vessels (E,F). (A) 5-week whole chorion ( $n=3$ ). (B) A small cluster of CD34<sup>+</sup> CD45<sup>+</sup> cells interacts with vimentin<sup>+</sup> stromal cells at the base of a villus in an 8-week whole chorion ( $n=2$ ). This section was visualized with differential interference contrast (DIC; grayscale). (C) CD34<sup>+</sup> CD45<sup>+</sup> cells in a 16-week CP ( $n=4$ ). (D) CD34<sup>+</sup> CD45<sup>+</sup> cells in a 23-week CP ( $n=3$ ). (E) CD34<sup>+</sup> CD45<sup>+</sup> cells of the SC from the same specimen shown in C ( $n=4$ ). (F) CD34<sup>+</sup> CD45<sup>+</sup> cells in the SC from the same specimen shown in D ( $n=3$ ). Nuclei were visualized by staining with DAPI. Confocal images were obtained by sequential scanning of stained tissue sections. Arrows (A,E) indicate the presence of cells coexpressing CD34 and CD45 antigens. Scale bars: 50  $\mu$ m.

5-8 weeks of gestation (Fig. 3B). In the first trimester, they gradually diminished to  $\sim 10^4$  cells/g and this density persisted for the rest of gestation. Although there was variability among samples, the total number of CD34<sup>++</sup> CD45<sup>low</sup> cells in the chorion substantially increased towards term (Fig. 3C): first trimester ( $n=21$ ),  $12\text{--}58 \times 10^3$  cells/tissue; second trimester ( $n=21$ ),  $1.0\text{--}21 \times 10^4$  cells/tissue; and third trimester ( $n=9$ ),  $0.8\text{--}15 \times 10^5$  cells/tissue. These data show that the density of CD34<sup>++</sup> CD45<sup>low</sup> cells was highest in the first trimester, whereas absolute numbers were highest at term. These findings are in line with our previous observations in chorionic villi of the human placenta (Barcena et al., 2009).

#### **CD34<sup>++</sup> CD45<sup>low</sup> cells in the chorion have a similar phenotypic profile to the equivalent intraembryonic population**

The antigenic profiles of the light-density chorion cells are shown in Fig. 4 ( $n=3$ ). At mid-gestation, there are abundant CD34<sup>-</sup> CD45<sup>+</sup> mature cells, mainly Hofbauer cells, and CD34<sup>-</sup> CD45<sup>-</sup> cells, mostly comprising stromal cells (data not shown). Analysis of CD34<sup>++</sup> CD45<sup>low</sup> cells (gated in Fig. 4A) showed that they express little CD38 and CD133 (PROM1), low levels of CD117 (KIT) and CD4, and medium to high levels of HLA-DR, CD31 (PECAM1),

CD90 (THY1), CD95 (FAS), TIE2 (TEK, CD202b, angiopoietin receptor 2) and CD71 (TFRC). These data suggest that the CD34<sup>++</sup> CD45<sup>low</sup> population is heterogeneous, possibly including both hematopoietic and endothelial lineage (TIE2<sup>+</sup>) cells (Fig. 4B). In addition, this population displayed variable levels of CD13 (ANPEP), CD33 and EPOR (data not shown) and did not coexpress KDR (VEGFR2, CD309) or CD150 (SLAMF1) (Fig. 4B). Thus, the CD34<sup>++</sup> CD45<sup>low</sup> cells in the chorion displayed a phenotypic profile similar to that of the most primitive subset (CD38<sup>-/low</sup>) of the intraembryonic counterpart population from fetal liver and bone marrow (BM), and was very similar to that of placental hematopoietic progenitors (Barcena et al., 2009; Bárcena et al., 1996; Muench et al., 1997).

#### **Transplantation of chorion cells into immunodeficient mice shows that they contain HSCs**

First, we identified the dissociation method that yielded the maximum number of repopulating HSCs. Collagenase digestion of the chorion failed to release cells that engrafted mice (Fig. 5A). Transplanted CD34<sup>++</sup> CD45<sup>low</sup> cells and their mature progeny (CD34<sup>-</sup> CD45<sup>+</sup> cells) were detected only after the chorion samples were subjected to serial enzymatic digestion by collagenase IA,

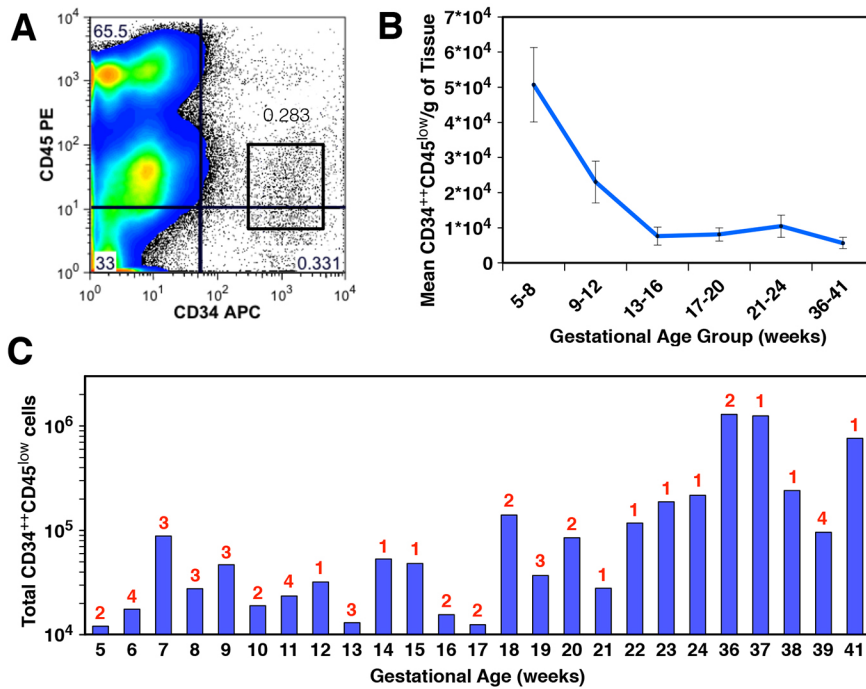


**Fig. 3. The density and total number of CD34<sup>++</sup> CD45<sup>low</sup> cells changes during development.** Light-density (LD) suspensions of human chorionic cells (SC+CP) were isolated and stained with monoclonal antibodies (mAbs) against CD34, CD45, as well as isotype-matched control mAbs. (A) Representative analysis of an 18-week chorion sample, showing the gate employed to determine the frequency of CD34<sup>++</sup> CD45<sup>low</sup> cells. (B) The density (mean number/g tissue) of CD34<sup>++</sup> CD45<sup>low</sup> cells at the indicated gestational windows (n=51; error bars indicate s.e.m.). (C) The total number of CD34<sup>++</sup> CD45<sup>low</sup> cells contained in chorion samples (n=51) at different gestational ages was calculated by multiplying the percentage of cells in the gate (shown in A) by the total number of cells (5-12 weeks) or the number of LD cells (13-41 weeks). The number of samples analyzed of each gestational age is indicated in red.

followed by trypsin (Fig. 5A). The level of human cell engraftment in the BM obtained with cells isolated using collagenase IA and trypsin was similar in both of the transplanted mice (~23%). The gating strategy employed to determine the frequency of human cells

is shown in Fig. S2A. Multilineage engraftment was observed in these mice, with 24-30% B cells (CD19<sup>+</sup>), 18-19% erythrocytes [CD235a (GYPA)<sup>+</sup>], 7-8% myeloid cells [CD14<sup>+</sup> and CD66b (CEACAM8)<sup>+</sup>], as well as 35-37% CD34<sup>+</sup> progenitor cells.

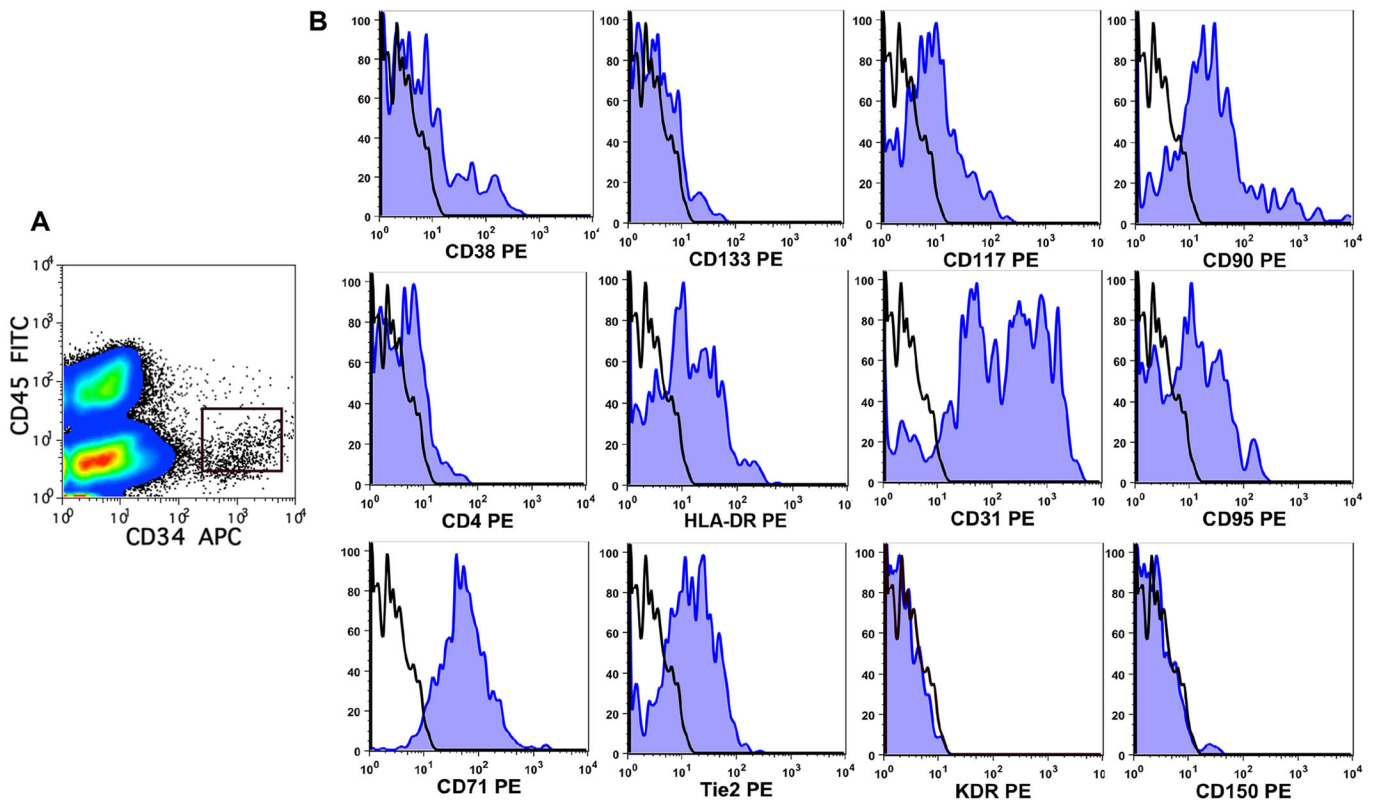


**Fig. 4. Phenotypic profile of chorionic CD34<sup>++</sup> CD45<sup>low</sup> cells.** (A) LD suspensions of human chorionic cells (19 weeks of gestation) were stained with the indicated mAbs and PI. 1 × 10<sup>6</sup> viable cells were acquired for each analysis to ensure that at least 4 × 10<sup>3</sup> events were included in the gate containing CD34<sup>++</sup> CD45<sup>low</sup> cells. (B) Expression of the indicated markers labeled with PE (blue); data from isotype-matched controls are outlined in black. This experiment is representative of three experiments that analyzed the full marker set and 17 that analyzed a subset of the panel.



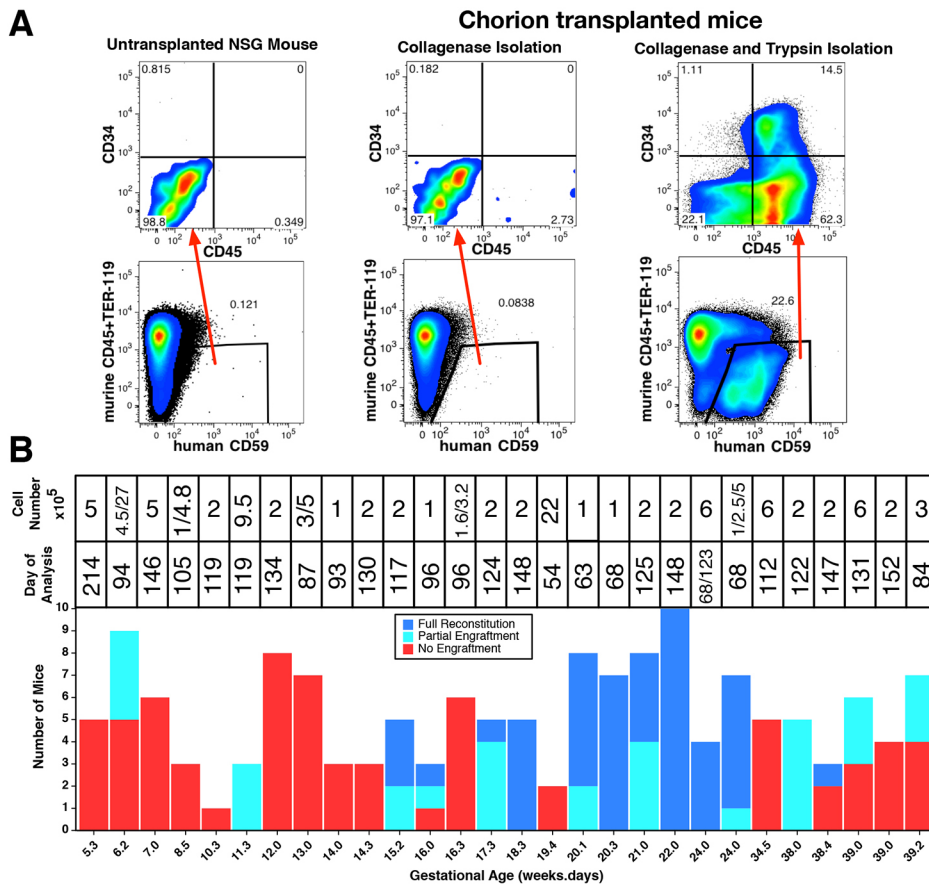


**Fig. 5. The engraftment potential of cells from the human chorion peaks at mid-gestation and it is enabled by digestion with trypsin and collagenase.** (A)  $6 \times 10^6$  cells from a 24-week specimen isolated using collagenase IA alone and  $6 \times 10^5$  cells isolated by the two-enzyme digestion method (trypsin and collagenase IA treatment) were transplanted into four mice and two mice, respectively. Engraftment was analyzed after 123 days with human cells defined by CD59 expression (see also Fig. S2A). (B) The number of full or partially engrafted mice, as well as those with no reconstitution, following transplantation with chorion of different gestational ages (5.3-39.2 weeks). The number of mice transplanted is indicated on the y-axis and gestational age is indicated in the x-axis ( $n=27$ ). Each bar represents a single experiment. The number of cells transplanted and the day of analysis are indicated above each bar.

We investigated the hematopoietic engraftment potential of chorionic cells of different gestational ages. The vast difference in the number of cells that can be obtained from first versus second trimester chorion samples prevented us from cell sorting specific populations (i.e.  $CD34^{++} CD45^{low}$ ) across all gestational ages. In addition, the low frequency of  $CD34^{++} CD45^{low}$  cells (0.01-1.9%) leads to very long cell sorts, which might affect cell purity and viability. Therefore, we transplanted unfractionated cell suspensions of enzymatically digested first trimester chorion samples and the light-density fraction of samples older than 12 weeks, which are enriched in  $CD34^{+}$  cells. In addition, for second trimester chorion samples ( $\geq 14$  weeks), lineage depletion ( $lin^{-}$ ) was performed (as described in the supplementary Materials and Methods). The transplanted cells were obtained by processing the entire CP and the SC together (second trimester) or 30-50 g of third trimester tissues. Five to ten mice were transplanted with each specimen of  $1-27 \times 10^5$  cells/mouse (first trimester),  $0.1-22 \times 10^5$  cells/mouse (second trimester) or  $2-6 \times 10^5$  cells/mouse (third trimester). Mice were analyzed from 9-30 weeks post-transplant, with the majority of analyses between 100 and 150 days. It has been reported that 7-10 weeks after transplant provides sufficient time to observe reconstitution derived from HSCs (Goyama et al., 2015; McKenzie et al., 2007), while more mature progenitors ( $CD38^{+}$ ) disappear by 4 weeks (Kerre et al., 2001). Mice transplanted with chorion cells obtained prior to 15 weeks of gestation showed no multilineage engraftment (Fig. 5B). In two cases, limited reconstitution by mostly myeloid- and/or T cells was observed in some or all of the mice (Fig. S3). With some variability, multilineage long-term hematopoietic reconstitution was detected from the fifteenth week of gestation onward (Fig. 5B). A general

absence of repopulating HSCs was observed from late pre-term (34 weeks, 5 days) and term (38-39 weeks) chorionic cells: only 1 out of 26 mice transplanted displayed full multilineage reconstitution, while 7 out of 26 mice had partial human engraftment (Fig. 5B). Our data showed that definitive HSCs are present in the chorion from 15 to 24 weeks, whereas prior to 15 weeks no HSC activity was detected, and during the third trimester HSCs were extremely rare. In Fig. S3 we provide more detail on the transplantation experiments summarized in Fig. 5B.

It is well established that HSCs occupy a hypoxic niche in the BM and that this environment maintains their repopulating potential and their quiescent state (Kubota et al., 2008). Accordingly, we performed colony-forming unit culture (CFU-C) assays in hypoxic (1%  $O_2$ ) and standard (20%  $O_2$ ) conditions with four chorionic samples of 5-10 weeks of gestation. We found that hematopoietic colony growth was not significantly affected by physiological hypoxia (Fig. S4A). Many non-hematopoietic colonies displaying fibroblast morphology were observed. The number of CFU-fibroblast obtained in hypoxic conditions was generally higher than in normoxic conditions (Fig. S4B). Based on these findings, we concluded that the lack of engraftment by early gestation samples could not simply be explained by a requirement for a low  $O_2$  environment.

**Chorionic HSCs generate multilineage progeny in immunodeficient mice and can be serially transplanted**

Multiparametric FACS analyses were performed on the BM, spleen and liver of animals engrafted with  $CD59^{+}$  second trimester  $lin^{-}$  chorion cells (22 weeks) using previously detailed methods (Varga et al., 2010). Total BM samples were analyzed to ensure the detection

of CD235a<sup>+</sup> erythrocytes, which were otherwise depleted during the isolation of light-density cells from spleen and liver samples. At 148 days post-transplant, the median level of human cell engraftment in the BM was 21.6% and ranged between 4.5 and 58% (*n*=10). Human chimerism was higher among splenocytes, which contained a median of 82% human cells (range 30.4-93.7%). Fig. 6 shows multilineage engraftment in a mouse with a high level of human chimerism. We used CD59 to identify all human cells, including mature CD235a<sup>+</sup> erythrocytes (Fig. S2B). CD45<sup>+</sup> leukocytes contained a substantial CD34<sup>+</sup> hematopoietic progenitor population. The human cells were at different stages of maturation, from HSCs (CD34<sup>++</sup> CD133<sup>+</sup>) and early progenitors (CD34<sup>++/+</sup>) to intermediate progenitors of the B-cell (CD34<sup>+</sup> CD19<sup>+</sup> cells), myeloid (CD34<sup>+</sup> CD33<sup>+</sup> cells) and erythroid (CD34<sup>+</sup> CD235a<sup>+</sup>) lineages. In addition, the BM of transplanted mice contained mature B cells (CD34<sup>-</sup> CD19<sup>+</sup>), mature myeloid cells (CD34<sup>-</sup> CD45<sup>+</sup> CD33<sup>+</sup>), erythrocytes (CD34<sup>-</sup> CD235a<sup>+</sup>), T cells (CD3<sup>+</sup>) and natural killer (NK) cells [CD56 (NCAM1)<sup>+</sup> CD3<sup>-</sup> CD7<sup>+</sup>]. In the spleen, we detected erythrocytes, monocytes (CD14<sup>+</sup> cells), platelets [CD41 (ITGA2B)<sup>+</sup> CD42b (GP1BA)<sup>+</sup>] and CD3<sup>+</sup> CD4<sup>+</sup> and CD3<sup>+</sup> CD8<sup>+</sup>

T cells. CD34<sup>++</sup> CD133<sup>+</sup> CD38<sup>-/low</sup> cells were also observed in the liver, consistent with previous observations that the adult mouse liver supports this primitive population of hematopoietic precursors (Muench et al., 2014).

To further verify long-term reconstitution by HSC engraftment, serial transplantation was performed in which the BM of primary recipients was transplanted into secondary recipients. Light-density lin<sup>-</sup> chorion cells from a 24-week sample were transplanted into two primary recipients and their BM was harvested 68 days later. Multilineage engraftment was observed in the BM of both mice, with frequencies of 43% or 53% human cells (data not shown). BM was pooled for transplantation into secondary recipients, which each received the equivalent of 36% of the BM content of a single femur. The BM of secondary recipients was analyzed after 92 days and contained 19-21% human cells (Fig. 7). The primitive progenitor population (CD34<sup>++</sup> CD133<sup>+</sup> CD38<sup>-/low</sup>) was readily detected, as well as B-cell progenitors, myeloid cells and erythrocytes. The myeloid population contained granulocytes (CD33<sup>+</sup> CD66b<sup>+</sup>) and monocytes (CD33<sup>+</sup> CD14<sup>+</sup>). In the spleen, platelets and T cells (single positive for CD4 or CD8) were present.

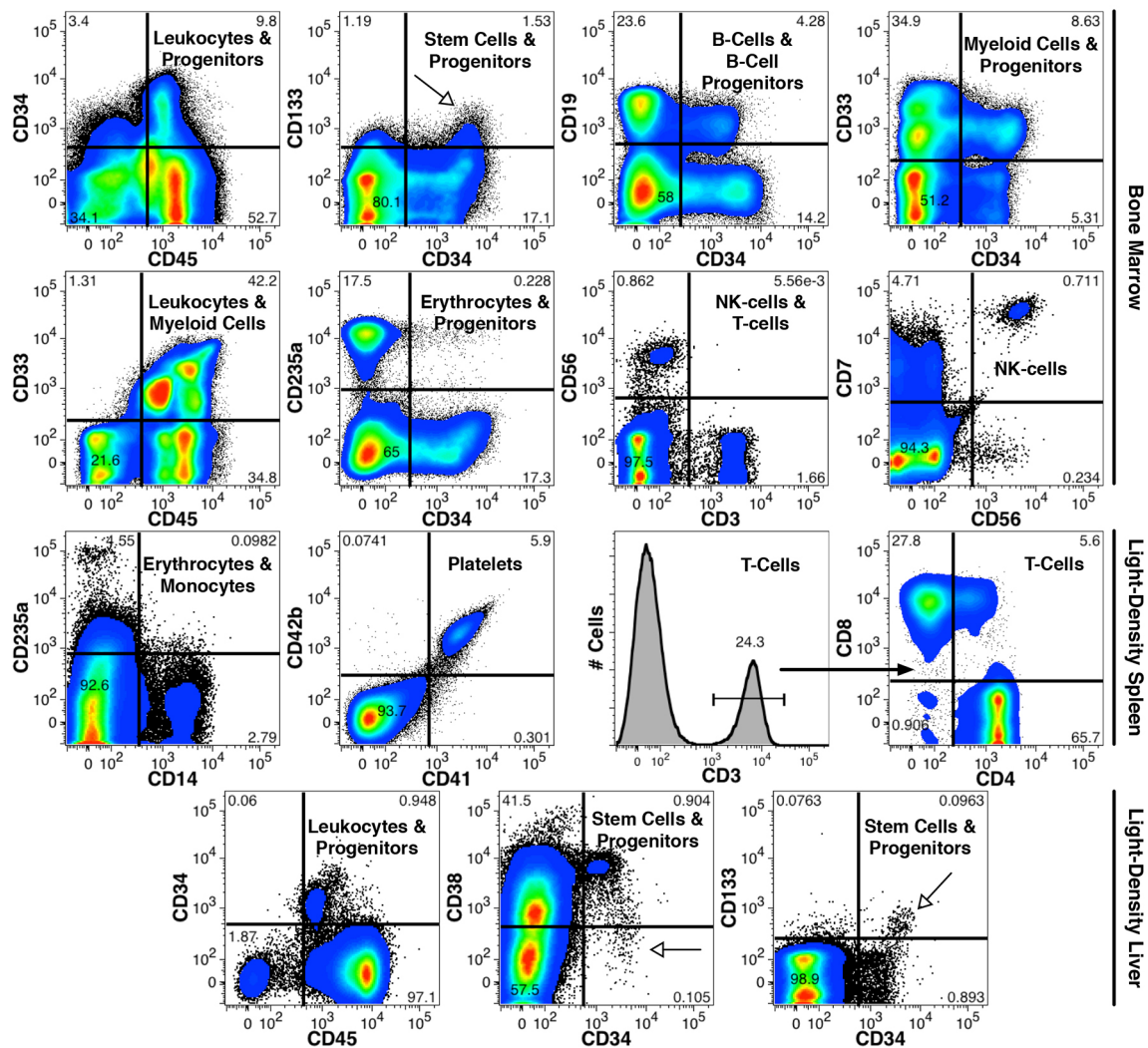


**Fig. 6. Multilineage engraftment by human chorionic cells in mice.** 2x10<sup>5</sup> LD, lin<sup>-</sup> chorionic cells at 22 weeks of gestation were transplanted into NSG mice and analyzed 148 days later. BM, spleen and liver were analyzed by FACS using the indicated mAbs. Human chimerism in total BM was 58%, as measured by the percentage of human CD59<sup>+</sup> cells that lacked strong expression of mouse markers. Open arrows indicate the likely HSC population. The different hematopoietic lineages detected among human CD59<sup>+</sup> cells engrafted in the mouse organs are labeled on these FACS plots, indicating multilineage reconstitution (*n*=10).



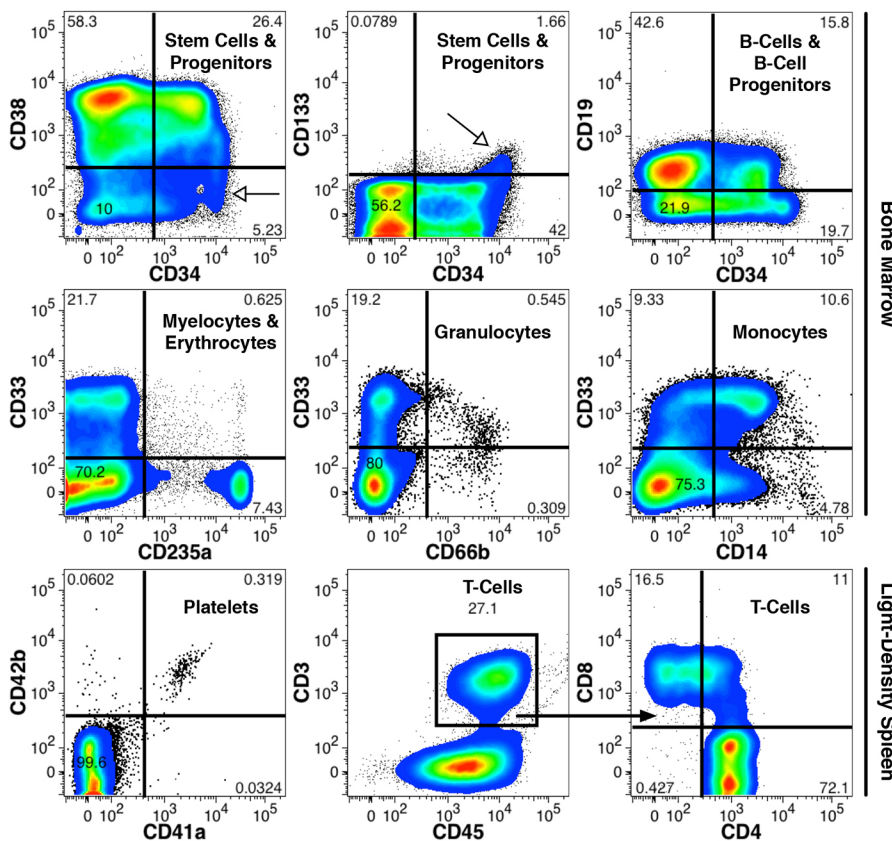


**Fig. 7. Chorionic cells engraft secondary recipients.** LD,  $lin^{-}$  human chorionic cells at 24 weeks of gestation were transplanted into mouse primary recipients. The BM was harvested 68 days later and re-transplanted. Total BM (top two rows) and LD spleen cells (bottom row) were analyzed 91 days after the second transplant. BM was engrafted with 21% human  $CD59^{+}$  cells. Analytical strategy and data depiction are similar to Fig. 6. Open arrows indicate the likely presence of an HSC population. The FACS results indicated multilineage serial reconstitution from primary to secondary recipients ( $n=2$ ).

These data demonstrate that the mid-gestation chorion contains HSCs capable of long-term, multilineage hematopoiesis with secondary transplant potential in adult hosts.

#### Extreme limiting-dilution analysis (ELDA) of chorion HSCs in immunodeficient mice

ELDA (Albelda et al., 1990) was performed to determine the frequency of HSCs among chorionic cells from two mid-gestation  $lin^{-}$  samples (20 weeks) (Hu and Smyth, 2009). Phenotypic analyses of the chorion cells prior to transplant showed that the frequency of potential HSCs ( $CD34^{++} CD45^{low} CD133^{+}$ ) was low (1-4 cells in  $1 \times 10^3$  cells of the light-density,  $lin^{-}$  fraction; data not shown). The estimated frequency of engrafted HSCs was 1 in  $3.3 \times 10^4$  light-density  $lin^{-}$  cells in one experiment (Fig. 8A) and 1 in  $8.2 \times 10^4$  light-density  $lin^{-}$  cells in the other (Fig. 8B). Using these values, we calculated that the transplantation of 33-132 (experiment 1) or 82-328 (experiment 2)  $CD34^{++} CD45^{low} CD133^{+}$  cells produced multilineage, long-term engraftment in mice. These frequencies are similar to those reported for human BM HSCs (Guezguez et al., 2013).

There is no universally agreed upon definition of engraftment as used as an indicator of HSC activity in immunodeficient mice. We used a strict definition to define full engraftment (presence of three lineages) that included detection of  $CD34^{+}$  cells as an indication of ongoing hematopoiesis, although failure to detect human red cells was often the cause of partial engraftment. Partial engraftment was detected in many mice in the limiting-dilution analyses in a pattern consistent with the dose of cells transplanted (Fig. 8C,D). As some of these mice may have been engrafted with HSCs but failed to achieve sufficient multilineage engraftment for detection, our estimate of HSC numbers might be low. In addition, the R-values

for the graphs shown in Fig. 8A,B were higher than 1, which implies that engraftment was hyper-responsive to dose. This behavior suggests multi-hit alternatives (Hu and Smyth, 2009), i.e. the presence of more than one cell population cooperating to produce full human cell reconstitution in mice or the cooperative effects of human hematopoietic cells in supporting their own growth and differentiation.

#### Sorted $CD34^{++} CD45^{low}$ chorion cells are of fetal origin and reconstitute immunodeficient mice

To determine the origin of HSCs residing in the chorion, we sorted  $CD34^{++} CD45^{low}$  cells from a CP plus SC whole-chorion sample obtained from a male at 18.3 weeks of gestation. Since the number of cells obtained was very low, we expanded them for 3.5 days *in vitro* in the presence of cytokines, after which we performed fluorescent *in situ* hybridization (FISH) with probes specific for the X or Y chromosomes. The results indicated that this population was of fetal origin, as 98% of the cells were male (Fig. 9A). Next, we sorted  $CD34^{++} CD45^{low}$  cells from a male SC sample at 23.6 weeks of gestation, and transplanted them into NSG-3GS mice ( $3 \times 10^3$  cells/mouse). After 61 days, multilineage human engraftment was observed in the BM, including erythroid, lymphoid (B, T and NK cells) and myeloid cells (Fig. 9B). The spleen contained human platelets and T cells (Fig. 9C), while the liver contained a  $CD34^{++} CD133^{+}$  HSC population (Fig. 9D). The BM from all four of the transplanted mice showed full human reconstitution and they were pooled to sort  $CD34^{++} CD45^{low}$  cells. FISH analysis showed that 100% of these cells were male (Fig. 9E). Identical results were obtained on sorted  $CD34^{-} CD45^{+}$  cells, demonstrating that the mature hematopoietic cells generated in the transplanted mice are also of fetal origin (data not shown). From these results we concluded that the HSC potential of the

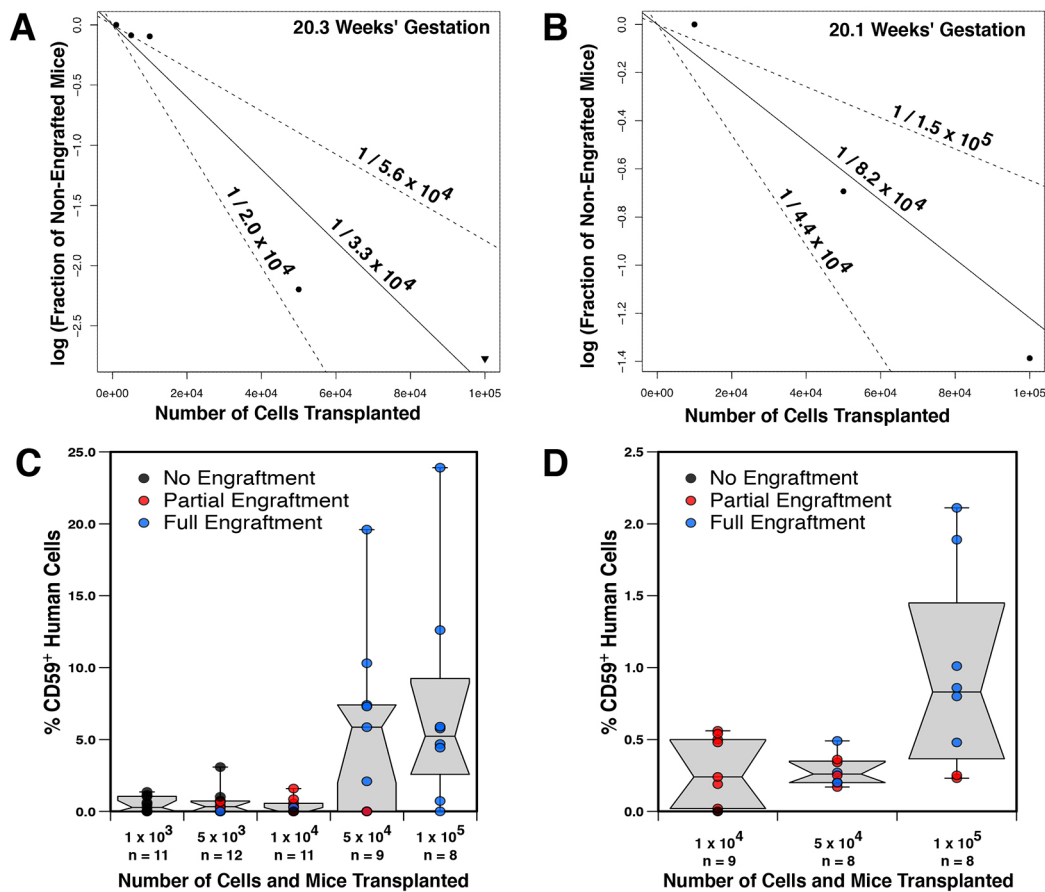


**Fig. 8. Enumeration of chorionic HSCs by ELDA.** Mice were transplanted with varying doses of LD,  $lin^{-}$  human chorionic cells isolated from two mid-gestation tissues, as indicated in the x-axis. Their BM was analyzed for human cells at 63 (A) and 68 (B) days post-transplant. ELDA was performed and the estimated frequency and range (95% confidence interval) of HSCs are indicated. Box plots of engraftment levels (percentage CD59<sup>+</sup> cells) for the experiments shown in A (C) and B (D). The results obtained from individual mice are shown in C,D, indicating partial, full or no multilineage engraftment.

chorion samples resides within the CD34<sup>++</sup> CD45<sup>low</sup> population and is not maternally derived.

#### Chemokine receptor and adhesion molecule expression of first and second trimester CD34<sup>++</sup> CD45<sup>low</sup> chorion cells

We asked whether functional differences among chorion HSCs before and after 15 weeks of gestation could be due to differential expression of chemokine receptors and adhesion molecules involved in homing to, and retention in, the mouse BM. We focused on chemokine receptors previously reported to be expressed by HSCs from human umbilical cord blood and BM (Aiuti et al., 1997; Basu and Broxmeyer, 2009; Broxmeyer et al., 2005; de Wynter et al., 1998; Lévesque et al., 2003; Peled et al., 2000; Rosu-Myles et al., 2000; Su et al., 1997; Tarnowski et al., 2010; Torossian et al., 2014). First trimester CD34<sup>++</sup> CD45<sup>low</sup> chorion cells expressed low levels of CXCR7 (ACKR3) and no detectable CD193 (CCR3) and CD195 (CCR5), but expression of the receptors increased in second trimester samples (Fig. 10A). Conversely, we detected CD191 (CCR1), which is expressed by CD34<sup>+</sup> cells in the human BM (de Wynter et al., 1998; Su et al., 1997), only on first trimester CD34<sup>++</sup> CD45<sup>low</sup> cells. These data suggest that the developmentally regulated expression of chemokine receptors could be responsible for the functional deficits of early gestation chorionic HSCs. In this context, the expression of CD191 alone failed to render functionally mature chorionic CD34<sup>++</sup> CD45<sup>low</sup> cells

capable of reconstitution. Instead, the cooperation among several chemokine pathways might be required for functional maturity in terms of homing.

Adhesion molecules are involved in HSC homeostasis, as they also regulate homing and retention of these cells to the BM niche. Thus, we asked whether chorionic CD34<sup>++</sup> CD45<sup>low</sup> cells expressed adhesion molecules that play crucial roles in these processes, specifically  $\beta 1$  integrins –  $\alpha 4\beta 1$  (VLA-4, CD49d, ITGA4),  $\alpha 5\beta 1$  (VLA-5, CD49e, ITGA5) and  $\alpha 6\beta 1$  (VLA-6, CD49f, ITGA6) – as HSCs with repopulating capacity express these receptors (Imai et al., 2010; Notta et al., 2011; van der Loo et al., 1998). Fig. 10B shows high expression of CD49d and CD49e and medium levels of CD49f during the first trimester. In comparison, second trimester chorionic CD34<sup>++</sup> CD45<sup>low</sup> cells lacked CD49d expression, displayed similar levels of CD49e and increased levels of CD49f. Other  $\beta 1$  integrins [ $\alpha 1\beta 1$  (CD49a, ITGA1),  $\alpha 2\beta 1$  (CD49b, ITGA2) and  $\alpha 3\beta 1$  (CD49c, ITGA3)] also implicated in BM adhesion were found to be expressed at similar levels regardless of gestational age (data not shown). Thus, the CD34<sup>++</sup> CD45<sup>low</sup> cells isolated from the first and second trimester chorion had different integrin expression profiles. Correlating these results with the *in vivo* transplantation data suggested that the downregulation of CD49d and the upregulation of CD49f might be important signals for the functional maturation of chorionic HSCs.



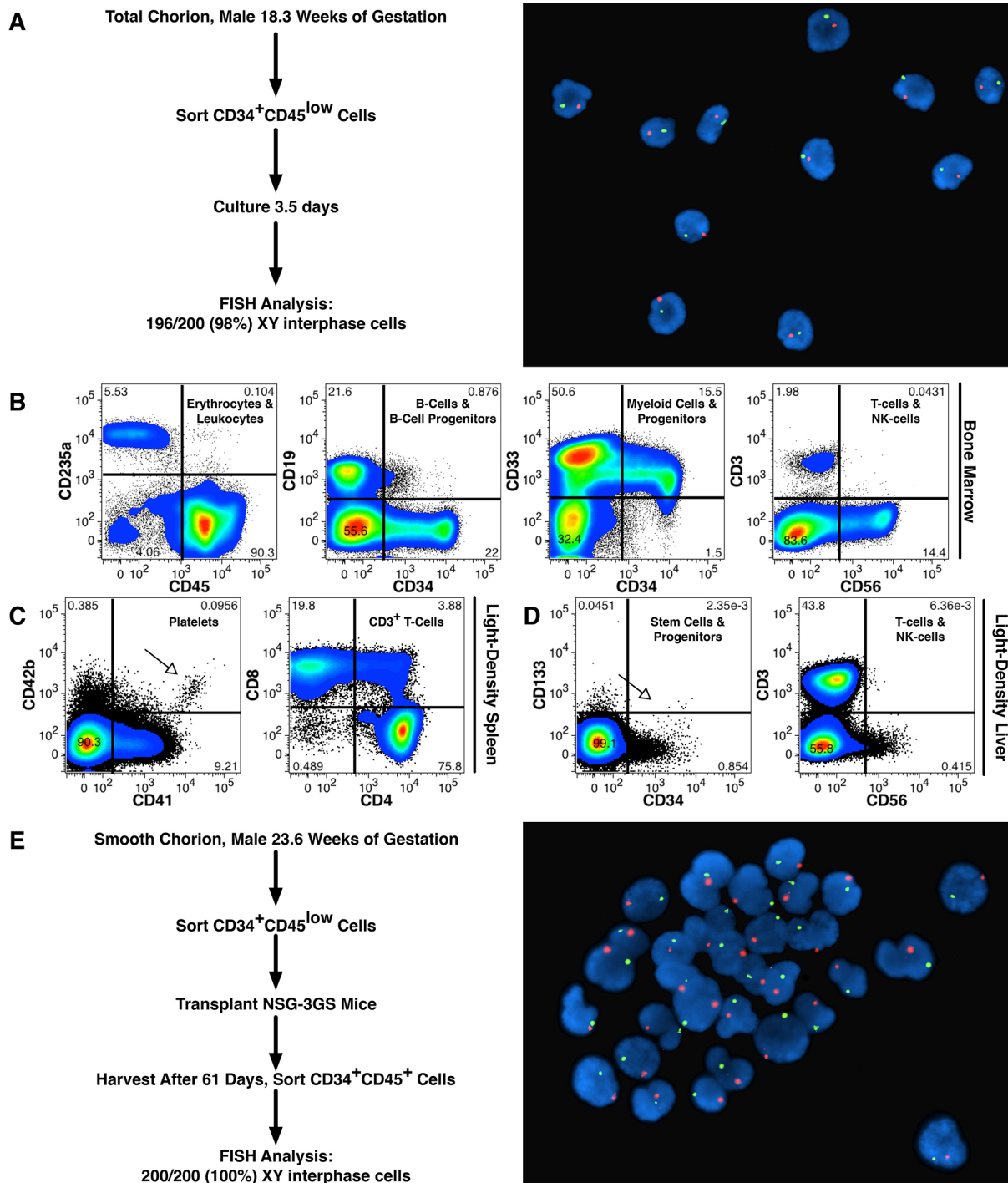


**Fig. 9. CD34<sup>++</sup> CD45<sup>low</sup> human chorionic cells are of fetal origin and contain HSCs.** (A)  $1 \times 10^4$  CD34<sup>++</sup> CD45<sup>low</sup> cells were isolated by FACS from the CP+SC of a male fetus at 18.3 weeks of gestation and cultured for 3.5 days. FISH analysis showed that 98% of the interphase cells had a male (XY) signal. A photomicrograph of the cells that were analyzed is shown (green, X chromosome; orange, Y chromosome). CD34<sup>++</sup> CD45<sup>low</sup> cells isolated from a male SC at 23.6 weeks of gestation were transplanted into NSG-3GS mice. Engraftment was analyzed 61 days later ( $n=4$ ). Representative results showing hematopoietic engraftment of the BM (B), spleen (C) and liver (D) are shown. Open arrows indicate splenic platelets (C) and a likely population of HSCs in the liver (D). (E) The BM of four engrafted mice was pooled and CD34<sup>++</sup> CD45<sup>+</sup> cells isolated by FACS, all of which were male as assessed by FISH analysis. A photomicrograph of CD34<sup>++</sup> CD45<sup>+</sup> cells sorted from the mouse BM cells showed a male (XY) signal.

**DISCUSSION**

Here we demonstrate the hematopoietic potential of the human chorion. It was previously reported that the mouse chorion possesses hematopoietic progenitors prior to the establishment of fetal circulation (Zeigler et al., 2006) or the chorio-allantoic fusion

(Corbel et al., 2007), thus pointing to the likely *in situ* generation of hematopoietic progenitors expressing *Runx1* and CD41. The notion that hematopoietic progenitors are engendered intrinsically in extraembryonic tissues was further supported by the finding of multilineage hematopoietic progenitors in mouse placenta of

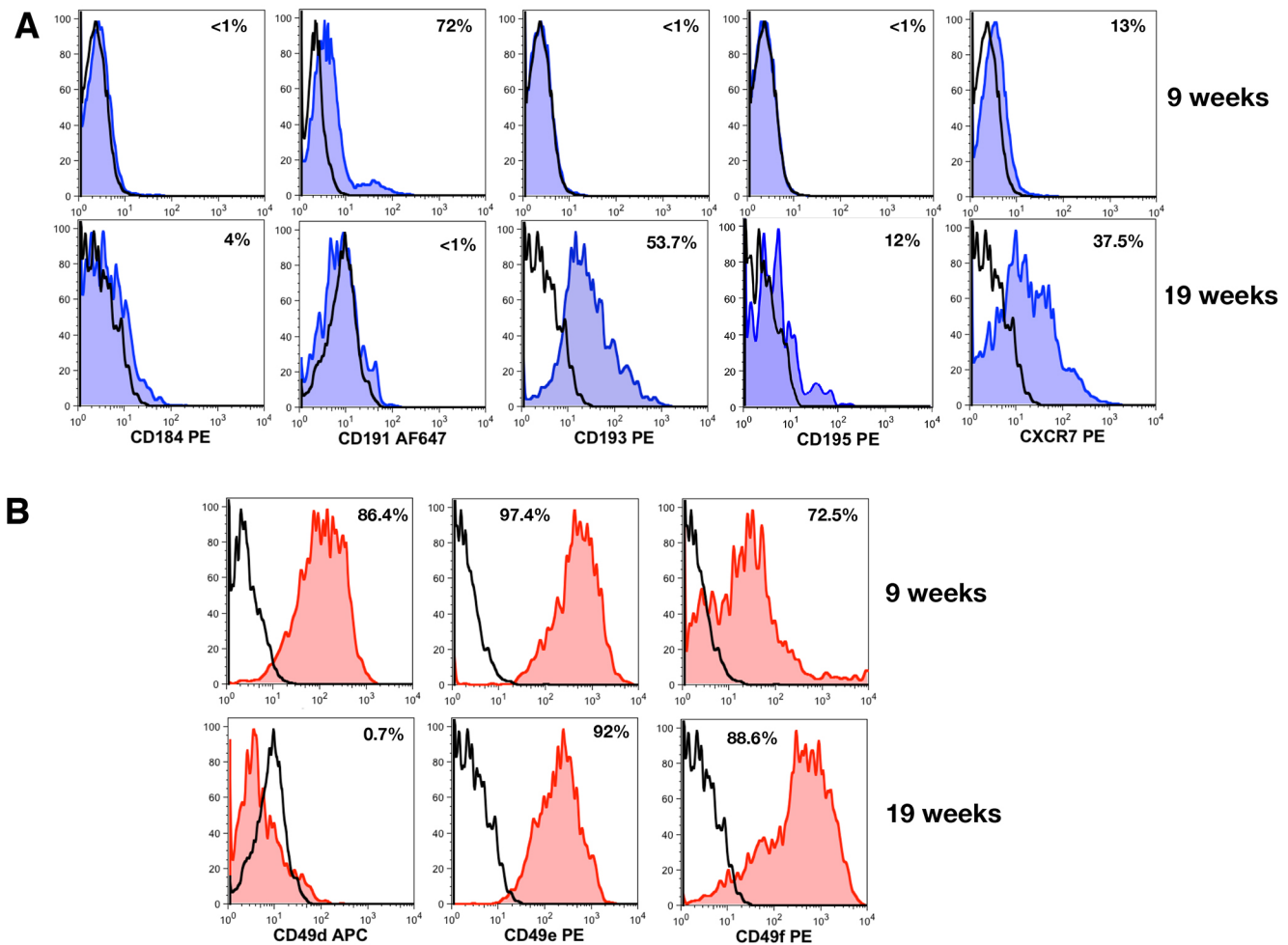


**Fig. 10. CD34<sup>++</sup> CD45<sup>low</sup> chorionic cells express several chemokine receptors and  $\beta$ 1 integrins.** (A) Freshly isolated LD suspensions of human chorionic cells from 9-week and 19-week samples were stained with the indicated mAbs and PI. Similar to the analysis performed in Fig. 4, a gate was set to include CD34<sup>++</sup> CD45<sup>low</sup> cells. Staining with mAbs against chemokine receptors (CD184, CD193, CD195, CXCR7 and CD191) and isotype-matched controls is shown. The expression of each marker in the PE and Alexa Fluor 647 (AF647) channels is shown (blue); data from isotype-matched control mAbs are outlined in black. This experiment is representative of the analysis of  $n=3$  for first trimester and  $n=4$  for second trimester samples. (B) LD suspensions of chorionic cells from the same 9-week and 19-week specimens were stained with the indicated mAbs and PI. A gate was set to include CD34<sup>++</sup> CD45<sup>low</sup> chorionic cells (not shown), and their staining with mAbs against CD49d ( $\alpha_4\beta_1$ ), CD49e ( $\alpha_5\beta_1$ ) and CD49f ( $\alpha_6\beta_1$ ) is shown in red, with the data from isotype-matched control mAbs outlined in black.  $n=6$ , three from the first and three from the second trimester.

*Ncx1*<sup>-/-</sup> (*Slc8a1*<sup>-/-</sup>) embryos, which lack heartbeat and, therefore, have no fetal blood circulation (Rhodes et al., 2008). These multipotent progenitors were able to produce erythroid, myeloid and lymphoid progeny *in vitro*. Although the self-renewing ability of mouse placental HSCs has been extensively documented (Gekas et al., 2005; Ottersbach and Dzierzak, 2005), the long-term repopulating activity of placental *Ncx1*<sup>-/-</sup> hematopoietic progenitors has not been addressed and whether the murine chorion contains HSCs remains unknown.

To our knowledge, this is the first demonstration of transplantable, definitive HSCs in the human chorion, which are absent in the amnion. Specifically, the chorion contains CD34<sup>++</sup> CD45<sup>low</sup> cells capable of long-term, multilineage reconstitution in mice and these cells could be serially transplanted into secondary recipients resulting in engraftment. By performing limiting-dilution transplantation studies, we estimated the frequency of HSCs to be 1 in  $3.3\text{--}8.2 \times 10^4$  light-density *lin*<sup>-</sup> cells. Taken together, our data demonstrated that the chorionic membrane provides an extraembryonic site of hematopoiesis during human gestation that harbors a resident population of HSCs, albeit at low frequency.

The primary goal of our study was to map the emergence and presence of hematopoietic precursors in the chorion during gestation. In line with our previously reported observations in placenta (Barcena et al., 2009), the early gestation chorion (5–8 weeks) contained higher numbers of CD34<sup>++</sup> CD45<sup>low</sup> cells/g tissue than observed later in development, although it is important to stress that this population of cells is always present at a low frequency (less than 1% of light-density chorion cells). Their density significantly drops from the ninth week onward, and is maintained at a constant level for the remainder of gestation. However, the transplantation of early gestational age chorion samples occasionally produced one or two hematopoietic lineages (e.g. unilineage T-cell reconstitution), but not multilineage engraftment in mice. By contrast, from the fifteenth week of gestation onward, the chorion consistently contained definitive HSCs. This observation resonates with a report by Ivanovs et al. (2011), in which the authors reported transient unilineage T-cell repopulation when transplanting early placentas (26–41 days of gestation) into immunodeficient mice; multilineage, long-term engraftment



was only accomplished when placentas of 15 weeks of gestation or older were transplanted.

The mechanisms that orchestrate changes in the functional status of extraembryonic HSCs as gestation advances are not known. Cells with the phenotype of hematopoietic progenitors that were isolated from early gestation tissues might possess limited potential and represent a primitive wave of hematopoietic progenitors unable to reconstitute mice. A potentially important player in the regulation of hematopoietic potential could be the hypoxic environment of extraembryonic tissues during early pregnancy. Since the placenta is not steadily perfused with maternal blood prior to 10-12 weeks of pregnancy (Rodesch et al., 1992), physiological hypoxia could play a role in regulating hematopoiesis. It has been suggested that HSCs in the BM reside in a hypoxic niche that maintains their repopulating potential and their quiescent state (Kubota et al., 2008), and hematopoietic tissues in the mouse embryo, such as the aorta-gonad-mesonephros (AGM) region, liver and placenta, are also hypoxic (Imanirad and Dzierzak, 2013). Likewise, the human chorion is poorly vascularized and possibly provides a hypoxic environment. We addressed the question of whether the oxygen level has a functional impact on early hematopoietic progenitors. Our data showed no consistent differences between CFU-C production at hypoxic versus normoxic conditions. However, we could not rule out the possibility that hypoxia may work indirectly via the niche, which is dismantled when we isolate the cells.

An alternative explanation for the age-related functional disparities among chorionic hematopoietic precursors could be differences in their homing abilities and/or adhesion properties. We focused on receptors that are expressed by perinatal and postnatal HSCs. Our study shows that there are important differences among first and second trimester chorionic CD34<sup>+</sup> CD45<sup>low</sup> cells with regards to their chemokine receptor expression profile. CD184 (CXCR4), the CXCL12 receptor, plays a crucial role in regulating HSCs homing to the BM (Aiuti et al., 1997; Broxmeyer et al., 2005; Lévesque et al., 2003; Peled et al., 2000). CD195 ligands (CCL3, CCL4 and CCL5) modulate the chemotaxis of CD34<sup>+</sup> cells in cord blood via the CD184-CXCL12 pathway (Basu and Broxmeyer, 2009). CD195 is expressed at higher levels on cord blood HSCs than on those obtained from BM or mobilized to peripheral blood (Rosu-Myles et al., 2000). CXCR7, another CXCL12 receptor (Tarnowski et al., 2010), cooperates with CD184 in enhancing the effects of CXCL12 on cell cycling, survival and proliferation of CD34<sup>+</sup> cells from peripheral blood (Torossian et al., 2014). In addition, CD34<sup>+</sup> cells from umbilical cord blood express CD193 (Lamkhioued et al., 2003), and CD191 expression by CD34<sup>+</sup> cells in cord blood confers superior engraftment of immunodeficient mice (de Wynter et al., 2001). Our data showed that first trimester chorionic progenitor cells express CD191 and low levels of CXCR7, features that do not render chorionic CD34<sup>+</sup> CD45<sup>low</sup> cells transplantable. Second trimester CD34<sup>+</sup> CD45<sup>low</sup> cells, although largely CD191<sup>-</sup>, consistently expressed CD184, CD193, CD195 and CXCR7. Therefore, transplantable second trimester chorionic HSCs share the chemokine receptor profile with HSCs from perinatal and postnatal origins.

Similarly, second trimester chorionic CD34<sup>+</sup> CD45<sup>low</sup> cells share many characteristics with fetal liver and fetal BM HSCs/progenitors [expression of CD133, CD117, CD4, HLA-DR, CD95 (Fig. 4) and CD13, CD33 (data not shown)]. Despite the commonalities, definitive chorionic CD34<sup>+</sup> CD45<sup>low</sup> cells display unique phenotypic properties, such as low-level CD38 expression and their  $\beta$ 1 integrin expression profile (CD49d<sup>-</sup> CD49e<sup>+</sup> CD49f<sup>+</sup>).

Second trimester fetal liver CD34<sup>+</sup> CD45<sup>low</sup> cells coexpress CD49d (data not shown) and contain transplantable HSCs (Muench et al., 2014). Therefore, CD49d expression does not correlate with functional HSCs in the chorion. We conclude that the adhesion and homing properties of the extraembryonic niche might differ from those of the intraembryonic counterpart.

The origin of human extraembryonic HSCs is uncertain. Here we employed a FISH approach on second trimester male chorion samples to establish the fetal origin of sorted CD34<sup>+</sup> CD45<sup>low</sup> cells, as well as to identify their progeny produced *in vivo*. Despite their fetal origin, CD34<sup>+</sup> CD45<sup>low</sup> cells could arise *in situ* to later populate the embryo/fetus. Alternatively, they might have an intraembryonic origin, colonizing extraembryonic structures once blood circulates. We cannot obtain chorion prior to 5 weeks of gestation and therefore, in all of our samples, the fetal-placental circulation was already established (Hamilton and Boyd, 1970). The AGM of 32-day-old human embryos (Carnegie stage 14) contains transplantable HSCs, preceding yolk sac, liver and placenta production of these cells (Ivanovs et al., 2011). Although suggestive, definitive proof that AGM-derived or liver-derived HSCs migrate to the placenta/chorion is lacking. Regardless, these extraembryonic structures could be sites of HSC generation. Our immunolocalization studies showed that the majority of the chorionic CD34<sup>+</sup> CD45<sup>low</sup> cells were embedded within vimentin<sup>+</sup> stromal cells rather than being associated with blood vessels, suggesting their possible origin from mesodermal progenitors in the stroma, which is derived from the extraembryonic mesoderm. This finding is in line with data from timed rescue of *Runx1* null mouse embryos, which showed that definitive, adult-type HSCs originate in the nascent extraembryonic mesoderm before the fetal liver initiates definitive hematopoiesis (Tanaka et al., 2012).

We conclude that two separate hematopoietic niches coexist in the chorion: a predominant mesenchymal niche and a less common perivascular niche. The functional relationship between these two hematopoietic niches or whether cells traffic between these locations remains to be determined. It would be very interesting to define, at a molecular level, the similarities and differences between the niches, which could provide functional insights into the regulatory networks of these two locations.

## MATERIALS AND METHODS

### Isolation of hematopoietic progenitors from the amnion, chorion and placenta

Human tissues were obtained anonymously with the approval of the University of California, San Francisco Committee on Human Research. All donors gave written informed consent. Samples from 5-24 weeks of gestation were from elective pregnancy terminations at San Francisco General Hospital. Full-term specimens collected at the time of delivery were from Moffitt-Long Hospital, University of California, San Francisco, CA, USA. The gestational ages of first trimester specimens were estimated based on crown-rump lengths, measured by ultrasonography. The gestational ages of second trimester specimens were estimated by foot length. The ages are expressed in weeks and days (e.g. 20.5 weeks means 20 weeks, 5 days).

Hematopoietic cells from chorion and amnion (separated from one another by manual dissection) were isolated as previously described (Barcena et al., 2009). Age group-specific tissue processing is described in detail in the supplemental Materials and Methods.

### Flow cytometry

Freshly isolated single-cell suspensions were stained with monoclonal antibodies (see Table S1) and analyzed using a two-laser FACSCalibur or three-laser LSR II cytometer (BD Biosciences). CellQuest (BD Biosciences) or FlowJo version 9.2 software was employed for analyses,

which focused on live cells using an electronic gate to identify propidium iodide (PI)<sup>-</sup> events.

### Human hematopoietic engraftment of mice

Animal studies were performed with the approval of the Institutional Animal Care and Use Committee at PMI Preclinical, San Carlos, CA, USA. Mice received humane care according to the criteria outlined by the National Academy of Sciences in the Guide for the Care and Use of Laboratory Animals as detailed in Varga et al. (2010). Founder NOD.Cg-*Prkdc<sup>scid</sup> Il2rg<sup>tm1Wjl</sup>/SzJ* (NSG) and NOD.Cg-*Prkdc<sup>scid</sup> Il2rg<sup>tm1Wjl</sup> Tg* (CMV-IL3,CSF2,KITLG)1Eav/MloySzJ (NSG-3GS) mice were obtained from Jackson Laboratories and maintained, bred and transplanted in a restricted-access, specific pathogen-free vivarium at Blood Systems Research Institute, San Francisco, CA, USA. For additional details on the transplantation of human cells into mice, as well as the harvest of mouse tissues for engraftment analyses, see the supplementary Materials and Methods.

Human chimerism in mice was studied between 63 and 214 days post-transplant; the majority of analyses were performed between 100 and 150 days. Mice were sacrificed by carbon dioxide asphyxiation followed by cervical dislocation. BM was harvested using a syringe with a 27-gauge needle to flush the femurs with ~3 ml culture medium. Spleen and liver specimens were held in culture medium on ice until cell isolation. At the conclusion of the experiment, mice were examined for signs of poor health or pathologies such as tumors of the liver, spleen and/or thymus. Any moribund animals were removed from the study. Mouse BM, spleen and liver were processed as previously described (Varga et al., 2010).

The frequency of live human cells in the transplanted mice was determined based on the percentage of CD59<sup>+</sup> cells that lacked the expression of mouse markers (Fig. S2). The presence of transplanted HSCs was determined by measuring engraftment of myeloid [CD33<sup>+</sup>, CD14<sup>+</sup>, CD66b<sup>+</sup> and/or CD15 (FUT4)<sup>+</sup> cells], erythroid (CD235a<sup>+</sup>), lymphoid (CD19<sup>+</sup> B cells, CD3<sup>+</sup> T cells and CD56<sup>+</sup> CD3<sup>-</sup> NK cells) and hematopoietic precursor (CD34<sup>+</sup> CD133<sup>+</sup> CD38<sup>-</sup>) cells by FACS. Engraftment of experimental mice was defined as a higher frequency of lineage marker-positive events in recipients as compared with control cells from an untransplanted mouse that were processed in parallel. Engraftment was defined as a minimum of five positive events above untransplanted controls. Full engraftment was defined as detection of all four cell types: myeloid, erythroid, lymphoid and precursors. Partial engraftment was defined as any engraftment less than full engraftment.

### Hematopoietic progenitor assays

To enumerate CFU-Cs, methylcellulose clonal cultures of chorion cell suspensions were plated at a density of  $2 \times 10^3/35$ -mm plate (BD Falcon, BD Biosciences) in Methocult GF H4435 (StemCell Technologies). Colonies containing myeloid cells or CFU-GM (CFU-granulocyte-macrophage progenitors) and CFU-mix (CFU-granulocyte-macrophage and erythroid cells) were scored after growth for 3.5 weeks at 37°C in normoxic (20% O<sub>2</sub>) or physiologically hypoxic (1% O<sub>2</sub>) conditions.

### Statistical analysis

For the estimation of HSC frequency in the mid-gestation chorion, ELDA (Albelda et al., 1990) was performed according to the method of Hu and Smyth (2009). We employed ELDA software (<http://bioinf.wehi.edu.au/software/elda/>) to graph the results, which are also shown as box and whisker plots; median chimerism levels are indicated by a notch in the box.

### Immunolocalization and fluorescence microscopy

Chorion tissue sections (20 μm) were fresh-fixed in 4% paraformaldehyde for 90 min and processed as previously described (Prakobphol et al., 2006). The tissue sections were stained with monoclonal antibodies against CD34 (directly conjugated to FITC; clone 581, IgG1, BD Biosciences/Pharmingen, 555821; 1:25), CD45 (clones 2B11+PD7/26, IgG1, Dako/Agilent, GA75161-2; 1:50) and vimentin (clone SP20, Abcam, Ab92545; 1:100). For controls and secondary antibodies, see the supplementary

Materials and Methods. Staining with DAPI in Vectashield mounting medium (Vector Laboratories) was used to visualize nuclei. Slides were imaged on a Leica DM 6000-CS microscope integrated with the Leica TCS SP5 confocal platform.

### Cell sorting of CD34<sup>++</sup> CD45<sup>low</sup> cells from the chorion

Once the light-density lin<sup>-</sup> single-cell suspensions were obtained from the chorion, the cells were stained with anti-CD34-APC (BD Biosciences, 555824) and anti-CD45-PE (Biolegend, 304008) monoclonal antibodies following manufacturer's recommendations and sorted in a FACSAria cell sorter (BD Biosciences) as previously described (Barcena et al., 2009).

### In vitro expansion of CD34<sup>++</sup> CD45<sup>low</sup> cells for FISH

$1 \times 10^4$  sorted CD34<sup>++</sup> CD45<sup>low</sup> cells from an 18.3-week chorion (CP+SC) specimen were cultured in 48-well plates (BD Falcon, BD Biosciences) in 0.5 ml Stem Span II medium (StemCell Technologies) supplemented with 50 ng/ml Kit ligand, 100 ng/ml FLT3 ligand, 20 ng/ml thrombopoietin and 20 ng/ml interleukin 3; all the cytokines were from Peprotech, except FLT3 ligand, which was purchased from ORF Genetics (Kopavogur, Iceland). After 3.5 days in culture at 37°C, 5% CO<sub>2</sub>, the cells were harvested, fixed and deposited on slides for FISH.

### FISH

$2-10 \times 10^3$  sorted cells were processed immediately after isolation and FISH was performed using X chromosome-specific [Vysis CEP X (DXZ1) SpectrumGreen] and Y chromosome-specific [CEP Y (DYZ3) SpectrumOrange] probes from Abbott Molecular following the manufacturer's protocol and as previously reported (Qi et al., 2015). For additional details, see the supplementary Materials and Methods. The cells were stained with DAPI II (Abbott Molecular) to visualize nuclei. FISH results were analyzed and documented using the CytoVision system (Leica).

### Acknowledgements

We thank the staff and faculty at San Francisco General Hospital Women's Options Center for assistance in the collection of early gestation extraembryonic tissues; Ms Jean Perry (RN MS NP, UCSF, Department of Obstetrics, Gynecology and Reproductive Sciences) for assistance in obtaining the equivalent tissues at term; Mr Gabriel A. Goldfien and Mr Jason Farrell for assisting in sample collection; and Ms Katharine Suttill (Senior Scientific Illustrator, Science/AAAS) for the drawing of a human fetus in Fig. 1A.

### Competing interests

The authors declare no competing or financial interests.

### Author contributions

A.B.: conception, design, execution and interpretation of the data. M.O.M. and M.K.: contributed equally to the design and execution of the experiments. A.G.G., M.E.F., A.I.B., K.L.P., Z.Q. and M.G.: execution of the experiments. H.S.: acquisition of samples. A.B., M.O.M. and S.J.F.: drafting or revising the article.

### Funding

This work was supported by grants from the National Blood Foundation (A.B.), the National Institutes of Health (R21HD055328 to A.B., 1P01 DK088760 to M.O.M., and 1R56 AI101130 to S.J.F.) and Blood Systems Inc. The content is solely the responsibility of the authors and does not necessarily represent the official views of the National Institute of Diabetes and Digestive and Kidney Diseases or the National Institutes of Health. A.G.G. and A.I.B. were supported by a Bridges to Stem Cell Training grant TB1-01188 from the California Institute of Regenerative Medicine. Deposited in PMC for release after 12 months.

### Supplementary information

Supplementary information available online at <http://dev.biologists.org/lookup/doi/10.1242/dev.138438.supplemental>

### References

- Aiuti, A., Webb, I. J., Bleul, C., Springer, T. and Gutierrez-Ramos, J. C. (1997). The chemokine SDF-1 is a chemoattractant for human CD34<sup>+</sup> hematopoietic progenitor cells and provides a new mechanism to explain the mobilization of CD34<sup>+</sup> progenitors to peripheral blood. *J. Exp. Med.* **185**, 111–120.
- Albelda, S. M., Oliver, P. D., Romer, L. H. and Buck, C. A. (1990). EndoCAM: a novel endothelial cell-cell adhesion molecule. *J. Cell Biol.* **110**, 1227–1237.



- Bárcena, A., Park, S. W., Banapour, B., Muench, M. O. and Mechetner, E. B.** (1996). Expression of Fas/CD95 and bcl-2 in primitive hematopoietic progenitors in the human fetal liver. *Blood* **88**, 2013-2025.
- Barcena, A., Muench, M. O., Kapidzic, M. and Fisher, S. J.** (2009). A new role for the human placenta as a hematopoietic site throughout gestation. *Reprod. Sci.* **16**, 178-187.
- Barcena, A., Muench, M. O., Kapidzic, M., Gormley, M., Goldfien, G. A. and Fisher, S. J.** (2011). Human placenta and chorion: potential additional sources of hematopoietic stem cells for transplantation. *Transfusion* **51** Suppl. 4, 94S-105S.
- Basu, S. and Broxmeyer, H. E.** (2009). CCR5 ligands modulate CXCL12-induced chemotaxis, adhesion, and Akt phosphorylation of human cord blood CD34+ cells. *J. Immunol.* **183**, 7478-7488.
- Benirschke, K., Kaufmann, P. and Baergen, R. N.** (2006). Anatomy and pathology of the placental membranes. In *Pathology of the Human Placenta*, pp. 249-307. New York: Springer.
- Bourne, G.** (1962). The foetal membranes. A review of the anatomy of normal amnion and chorion and some aspects of their function. *Postgrad. Med. J.* **38**, 193-201.
- Broxmeyer, H. E., Orschell, C. M., Clapp, D. W., Hangoc, G., Cooper, S., Plett, P. A., Liles, W. C., Li, X., Graham-Evans, B., Campbell, T. B. et al.** (2005). Rapid mobilization of murine and human hematopoietic stem and progenitor cells with AMD3100, a CXCR4 antagonist. *J. Exp. Med.* **201**, 1307-1318.
- Corbel, C., Salaün, J., Belo-Diabangouaya, P. and Dieterlen-Lièvre, F.** (2007). Hematopoietic potential of the pre-fusion allantois. *Dev. Biol.* **301**, 478-488.
- Cross, J. C.** (1998). Formation of the placenta and extraembryonic membranes. *Ann. N. Y. Acad. Sci.* **857**, 23-32.
- de Wynter, E. A., Durig, J., Cross, M. A., Heyworth, C. M. and Testa, N. G.** (1998). Differential response of CD34+ cells isolated from cord blood and bone marrow to MIP-1 alpha and the expression of MIP-1 alpha receptors on these immature cells. *Stem Cells* **16**, 349-356.
- de Wynter, E. A., Heyworth, C. M., Mukaida, N., Matsushima, K. and Testa, N. G.** (2001). NOD/SCID repopulating cells but not LTC-1C are enriched in human CD34+ cells expressing the CCR1 chemokine receptor. *Leukemia* **15**, 1092-1101.
- Gekas, C., Dieterlen-Lièvre, F., Orkin, S. H. and Mikkola, H. K. A.** (2005). The placenta is a niche for hematopoietic stem cells. *Dev. Cell* **8**, 365-375.
- Goyama, S., Wunderlich, M. and Mulloy, J. C.** (2015). Xenograft models for normal and malignant stem cells. *Blood* **125**, 2630-2640.
- Guezguez, B., Campbell, C. J. V., Boyd, A. L., Karanu, F., Casado, F. L., Di Cresce, C., Collins, T. J., Shapovalova, Z., Xenocostas, A. and Bhatia, M.** (2013). Regional localization within the bone marrow influences the functional capacity of human HSCs. *Cell Stem Cell* **13**, 175-189.
- Hamilton, W. J. and Boyd, J. D.** (1960). Development of the human placenta in the first three months of gestation. *J. Anat.* **94**, 297-328.
- Hamilton, W. J. and Boyd, J. D.** (1970). *The Human Placenta*. Cambridge: Heffer and Sons.
- Hu, Y. and Smyth, G. K.** (2009). ELDA: extreme limiting dilution analysis for comparing depleted and enriched populations in stem cell and other assays. *J. Immunol. Methods* **347**, 70-78.
- Ilancheran, S., Moodley, Y. and Manuelpillai, U.** (2009). Human fetal membranes: a source of stem cells for tissue regeneration and repair? *Placenta* **30**, 2-10.
- Imai, Y., Shimaoka, M. and Kurokawa, M.** (2010). Essential roles of VLA-4 in the hematopoietic system. *Int. J. Hematol.* **91**, 569-575.
- Imanirad, P. and Dzierzak, E.** (2013). Hypoxia and HIFs in regulating the development of the hematopoietic system. *Blood Cells Mol. Dis.* **51**, 256-263.
- Ivanovs, A., Rybtsov, S., Welch, L., Anderson, R. A., Turner, M. L. and Medvinsky, A.** (2011). Highly potent human hematopoietic stem cells first emerge in the intraembryonic aorta-gonad-mesonephros region. *J. Exp. Med.* **208**, 2417-2427.
- Kerre, T. C. C., De Smet, G., De Smedt, M., Offner, F., De Bosscher, J., Plum, J. and Vandekerckhove, B.** (2001). Both CD34+38+ and CD34+38- cells home specifically to the bone marrow of NOD/LtSz scid/scid mice but show different kinetics in expansion. *J. Immunol.* **167**, 3692-3698.
- Kubota, Y., Takubo, K. and Suda, T.** (2008). Bone marrow long label-retaining cells reside in the sinusoidal hypoxic niche. *Biochem. Biophys. Res. Commun.* **366**, 335-339.
- Lamkhioued, B., Abdelilah, S. G., Hamid, Q., Mansour, N., Delespesse, G. and Renzi, P. M.** (2003). The CCR3 receptor is involved in eosinophil differentiation and is up-regulated by Th2 cytokines in CD34+ progenitor cells. *J. Immunol.* **170**, 537-547.
- Lévesque, J.-P., Hendy, J., Takamatsu, Y., Simmons, P. J. and Bendall, L. J.** (2003). Disruption of the CXCR4/CXCL12 chemotactic interaction during hematopoietic stem cell mobilization induced by G-CSF or cyclophosphamide. *J. Clin. Invest.* **111**, 187-196.
- Luckett, W. P.** (1975). The development of primordial and definitive amniotic cavities in early Rhesus monkey and human embryos. *Am. J. Anat.* **144**, 149-167.
- Mayani, H., Dragowska, W. and Lansdorp, P. M.** (1993). Characterization of functionally distinct subpopulations of CD34+ cord blood cells in serum-free long-term cultures supplemented with hematopoietic cytokines. *Blood* **82**, 2664-2672.
- McKenzie, J. L., Takenaka, K., Gan, O. I., Doedens, M. and Dick, J. E.** (2007). Low rhodamine 123 retention identifies long-term human hematopoietic stem cells within the Lin-CD34+CD38- population. *Blood* **109**, 543-545.
- Muench, M. O., Roncarolo, M. G. and Namikawa, R.** (1997). Phenotypic and functional evidence for the expression of CD4 by hematopoietic stem cells isolated from human fetal liver. *Blood* **89**, 1364-1375.
- Muench, M. O., Beyer, A. I., Fomin, M. E., Thakker, R., Mulvaney, U. S., Nakamura, M., Suemizu, H. and Bárcena, A.** (2014). The adult livers of immunodeficient mice support human hematopoiesis: evidence for a hepatic mast cell population that develops early in human ontogeny. *PLoS ONE* **9**, e97312.
- Notta, F., Doulatov, S., Laurenti, E., Poepll, A., Jurisica, I. and Dick, J. E.** (2011). Isolation of single human hematopoietic stem cells capable of long-term multilineage engraftment. *Science* **333**, 218-221.
- Ottersbach, K. and Dzierzak, E.** (2005). The murine placenta contains hematopoietic stem cells within the vascular labyrinth region. *Dev. Cell* **8**, 377-387.
- Peled, A., Kollet, O., Ponomaryov, T., Petit, I., Franitza, S., Grabovsky, V., Slav, M. M., Nagler, A., Lider, O., Alon, R. et al.** (2000). The chemokine SDF-1 activates the integrins LFA-1, VLA-4, and VLA-5 on immature human CD34(+) cells: role in transendothelial/stromal migration and engraftment of NOD/SCID mice. *Blood* **95**, 3289-3296.
- Prakobphol, A., Genbacev, O., Gormley, M., Kapidzic, M. and Fisher, S. J.** (2006). A role for the L-selectin adhesion system in mediating cytotrophoblast emigration from the placenta. *Dev. Biol.* **298**, 107-117.
- Qi, Z., Jeng, L. J. B., Slavotinek, A. and Yu, J.** (2015). Haploinsufficiency and triploinsensitivity of the same 6p25.1p24.3 region in a family. *BMC Med. Genomics* **8**, 38.
- Rhodes, K. E., Gekas, C., Wang, Y., Lux, C. T., Francis, C. S., Chan, D. N., Conway, S., Orkin, S. H., Yoder, M. C. and Mikkola, H. K. A.** (2008). The emergence of hematopoietic stem cells is initiated in the placental vasculature in the absence of circulation. *Cell Stem Cell* **2**, 252-263.
- Robin, C., Bollerot, K., Mendes, S., Haak, E., Crisan, M., Cerisoli, F., Lauw, I., Kaimakis, P., Jorna, R., Vermeulen, M. et al.** (2009). Human placenta is a potent hematopoietic niche containing hematopoietic stem and progenitor cells throughout development. *Cell Stem Cell* **5**, 385-395.
- Rodesch, F., Simon, P., Donner, C. and Jauniaux, E.** (1992). Oxygen measurements in endometrial and trophoblastic tissues during early pregnancy. *Obstet. Gynecol.* **80**, 283-285.
- Rosu-Myles, M., Khandaker, M., Wu, D. M., Keeney, M., Foley, S. R., Howson-Jan, K., Yee, I. C., Fellows, F., Kelvin, D. and Bhatia, M.** (2000). Characterization of chemokine receptors expressed in primitive blood cells during human hematopoietic ontogeny. *Stem Cells* **18**, 374-381.
- Serikov, V., Hounshell, C., Larkin, S., Green, W., Ikeda, H., Walters, M. C. and Kuypers, F. A.** (2009). Human term placenta as a source of hematopoietic cells. *Exp. Biol. Med.* **234**, 813-823.
- Su, S., Mukaida, N., Wang, J., Zhang, Y., Takami, A., Nakao, S. and Matsushima, K.** (1997). Inhibition of immature erythroid progenitor cell proliferation by macrophage inflammatory protein-1alpha by interacting mainly with a C-C chemokine receptor, CCR1. *Blood* **90**, 605-611.
- Tanaka, Y., Hayashi, M., Kubota, Y., Nagai, H., Sheng, G., Nishikawa, S.-I. and Samokhvalov, I. M.** (2012). Early ontogenic origin of the hematopoietic stem cell lineage. *Proc. Natl. Acad. Sci. USA* **109**, 4515-4520.
- Tarnowski, M., Liu, R., Wysoczynski, M., Ratajczak, J., Kucia, M. and Ratajczak, M. Z.** (2010). CXCR7: a new SDF-1-binding receptor in contrast to normal CD34(+) progenitors is functional and is expressed at higher level in human malignant hematopoietic cells. *Eur. J. Haematol.* **85**, 472-483.
- Torossian, F., Anginot, A., Chabanon, A., Clay, D., Guerton, B., Desterke, C., Boutin, L., Marullo, S., Scott, M. G. H., Lataillade, J.-J. et al.** (2014). CXCR7 participates in CXCL12-induced CD34+ cell cycling through beta-arrestin-dependent Akt activation. *Blood* **123**, 191-202.
- van der Loo, J. C., Xiao, X., McMillin, D., Hashino, K., Kato, I. and Williams, D. A.** (1998). VLA-5 is expressed by mouse and human long-term repopulating hematopoietic cells and mediates adhesion to extracellular matrix protein fibronectin. *J. Clin. Invest.* **102**, 1051-1061.
- Varga, N. L., Barcena, A., Fomin, M. E. and Muench, M. O.** (2010). Detection of human hematopoietic stem cell engraftment in the livers of adult immunodeficient mice by an optimized flow cytometric method. *Stem Cell Stud.* **1**, e5.
- Zeigler, B. M., Sugiyama, D., Chen, M., Guo, Y., Downs, K. M. and Speck, N. A.** (2006). The allantois and chorion, when isolated before circulation or chorio-allantoic fusion, have hematopoietic potential. *Development* **133**, 4183-4192.

## Supplemental Data

### Supplemental Methods

*Tissue processing.* Samples of chorion comprised both the smooth chorion (SC) and the chorionic plate (CP), which was denuded of chorionic villi (Fig. S1A and B), unless otherwise specified that only the SC was used (Fig.9). Once that the tissues were dissected under a microscope, we processed them following a method previously described (Genbacev et al., 2011) that we modified to improve the recovery of hematopoietic cells (Barcena et al., 2009). Specifically, we added a final enzymatic digestion treatment of the chorion, amnion and chorionic villi preparations with 181 U/ml collagenase I-A, 0.12 mg/ml DNase I, 0.70 mg/ml hyaluronidase type I-S, and 1 mg/ml BSA in PBS at 37°C. Digestion continued for 5-60 min until total cellular dissociation was observed. For tissues 5-6 wks of gestational age, it was not possible to separate the membrane portion from the placental chorionic villi, therefore we prepared cells from whole chorion. In older specimens ( $\geq 7$  wks) the CP was dissected from chorionic villi and those tissues were prepared separately. For 7-12 wks specimens, transplantation and FACS were performed on the dissociated cells without further fractionation. For samples older than 12 wks, the light-density (LD) fraction was obtained (by centrifugation over Nycoprep (1.077 g/ml; Greiner Bio-One, Monroe, NC) for 30 min (25°C) at  $600 \times g$ ) for FACS and transplantation, as previously described (Barcena et al., 2009). For older samples ( $\geq 14$  wks) in which the amnion has begun to fuse to the chorion, manual separation of these two membranes was performed, as shown macroscopically in Fig S1C and at a histological level in Fig. S1D and E (before and after amnion removal, respectively). This step was followed by enzymatic dissociation and isolation of the LD fraction was then subjected to our standard mature lineage(lin) depletion to enrich in hematopoietic progenitors prior to transplantation. The mAbs used for depletion were all unconjugated and obtained from BioLegend (San Diego, CA), used at  $1\mu\text{g}/10^6$  target cells, and recognized CD235a (erythrocytes), CD14 (macrophages), CD19 and CD29 (B cells), CD3 (T cells) and CD56 (NK cells). After washing to remove the excess unbound mAbs, the cells were subjected to negative magnetic selection by using BioMag magnetic beads coated with goat anti-mouse IgG antibody (Qiagen Inc., Germantown, MD). The resulting LD lin<sup>-</sup> cell suspension was

counted and transplanted into mice. For FACS analyses, no lineage depletions were performed.

*Human hematopoietic engraftment of mice.* NSG-3GS mice were only used for the transplant experiment associated with the FISH analyses shown in Fig. 9; NSG mice were used in all other experiments. Mice were irradiated with 175 or 200 cGy using an RS2000 X-Ray Biological Irradiator (RAD Source Technologies, Inc., Alpharetta, GA, USA) 1 to 3 hours before the procedure. Female and male mice were transplanted as adults ( $\geq 8$  wks old) by tail-vein injection using a 28g U100 insulin syringe (BD, Franklin Lakes, NJ, USA). The cells were suspended in 200  $\mu$ L of PBS (Mediatech, Inc., Manassas, VA, USA). For several days before and for the first month after transplant, the standard chow was replaced with irradiated Global 2018 rodent diet with 4100 ppm Uniprim<sup>®</sup> (Harlan Laboratories, Inc., Hayward, CA, USA). Most of the transplanted mice were analyzed between 100 and 150 days post-transplant. Mice were sacrificed by carbon dioxide asphyxiation followed by cervical dislocation. BM was harvested by using a syringe with a 27-gauge needle to flush the femurs with approximately 3 ml of culture medium as described (Mahajan et al., 2015). Spleen and liver specimens were held in culture medium on ice until cell isolation. At the conclusion of each experiment, mice were examined for signs of poor health or pathologies such as tumors of the liver, spleen, and/or thymus. Any moribund animals were removed from the study. Mouse BM, spleen and liver were processed as previously described (Varga et al., 2010).

*Immunolocalization and fluorescence microscopy.* We applied previously reported methods (Prakobphol et al., 2006). The binding of antibodies that were not direct conjugates was detected by using the appropriate species-specific secondary antibody, a rhodamine-conjugated donkey anti-mouse IgG for anti-CD45 (Jackson ImmunoResearch Laboratories Inc., West Grove, PA) and AF 633-conjugated goat-anti-rabbit IgG for anti-vimentin (Invitrogen). As controls, serial sections were stained with the secondary antibody alone or mouse-IgG<sub>1</sub>-FITC (BD Pharmingen).

*FISH.* In brief,  $2-10 \times 10^3$  sorted cells were placed in ice cold fresh fixative (v/v 3:1 methanol:acetic acid) for 30 minutes at 4°C. Then the cells were dropped onto a slide and dried under controlled conditions (25°C, 38% relative humidity). We performed FISH using X- and Y-chromosome specific probes following manufacturer's protocol



(Abbott Molecular) and methods we have previously reported (Qi et al., 2015).

## Supplemental References

**Barcena, A., Muench, M. O., Kapidzic, M. and Fisher, S. J.** (2009). A new role for the human placenta as a hematopoietic site throughout gestation. *Reprod Sci* **16**, 178-187.

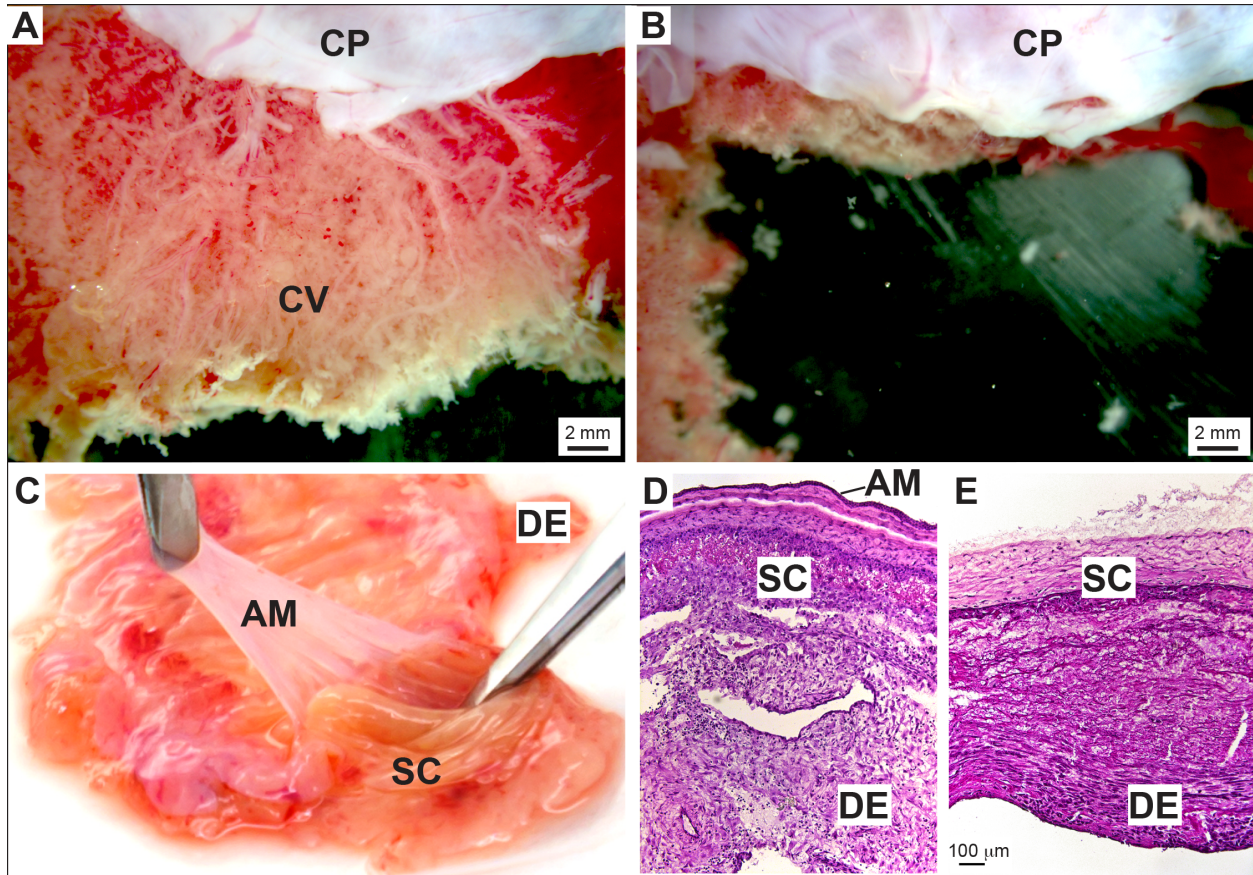
**Genbacev, O., Donne, M., Kapidzic, M., Gormley, M., Lamb, J., Gilmore, J., Larocque, N., Goldfien, G., Zdravkovic, T., McMaster, M. T., et al.** (2011). Establishment of human trophoblast progenitor cell lines from the chorion. *Stem Cells* **29**, 1427-1436.

**Mahajan, M. M., Cheng, B., Beyer, A. I., Mulvaney, U. S., Wilkinson, M. B., Fomin, M. E. and Muench, M. O.** (2015). A quantitative assessment of the content of hematopoietic stem cells in mouse and human endosteal-bone marrow: a simple and rapid method for the isolation of mouse central bone marrow. *BMC Hematol* **15**, 9.

**Prakobphol, A., Genbacev, O., Gormley, M., Kapidzic, M. and Fisher, S. J.** (2006). A role for the L-selectin adhesion system in mediating cytotrophoblast emigration from the placenta. *Dev Biol* **298**, 107-117.

**Qi, Z., Jeng, L. J., Slavotinek, A. and Yu, J.** (2015). Haploinsufficiency and triploinsensitivity of the same 6p25.1p24.3 region in a family. *BMC Med Genomics* **8**, 38.

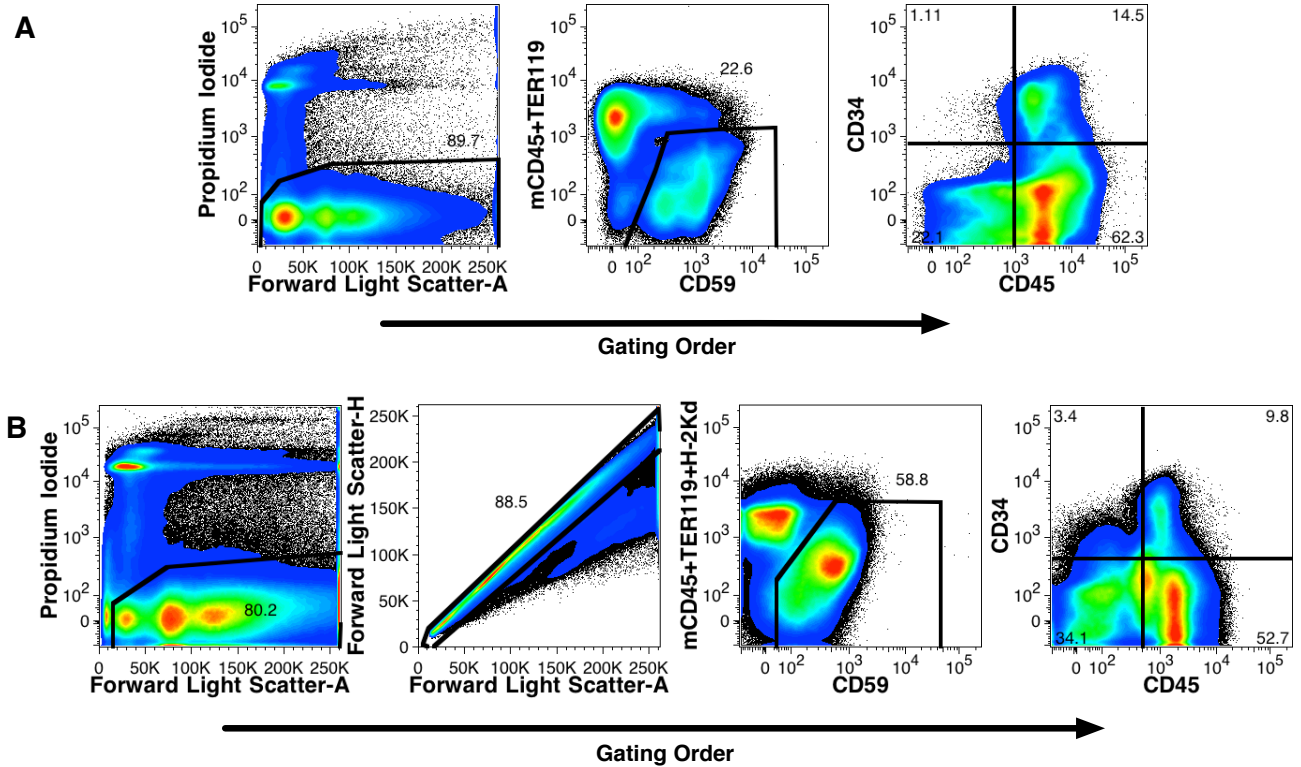
**Varga, N. L., Barcena, A., Fomin, M. E. and Muench, M. O.** (2010). Detection of human hematopoietic stem cell engraftment in the livers of adult immunodeficient mice by an optimized flow cytometric method. *Stem Cell Stud* **1**.



**Supplemental Figure S1. Dissection and histology of the fetal human membranes.**

**A.** A portion of the chorionic plate (CP) of a 19 wk specimen is visualized under a dissection microscope and is shown intact (with the chorionic villi (CV) attached). After dissecting the CV, we obtain the denuded chorion, which is the CP without the CV (**B**).

**C.** Manual separation of the amnion (AM) from the smooth chorion (SC) of a 22 wk specimen. A tissue section of the 22 wk amniochorion stained with hematoxylin and eosin is shown prior the removal of the amnion (**D**) and after the removal of the amnion (**E**). On the maternal side of the fetal membrane is the decidua (DE), which is manually removed prior the cell isolation.

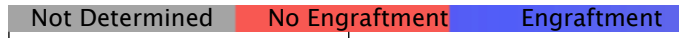


**Supplemental Figure S2. Complete gating strategy used to define human cells in mouse BM.** **A.** Live human cells were defined by their expression of CD59 and lack of expression of mouse markers, as well as the lack of propidium iodide staining as indicated in the gates. In some early studies the mouse markers were limited to CD45 and TER119, whereas the class I major histocompatibility antigen H-2k<sup>d</sup> was stained in later experiments to further stain non-hematopoietic cells of mouse origin (**B**). Additionally, the use of forward-light scatter area (A) and height (H) parameters to exclude doublets was employed in some later analyses. Data shown correspond to engraftment data shown in Figs. 5A (**A**) and 6 (**B**).

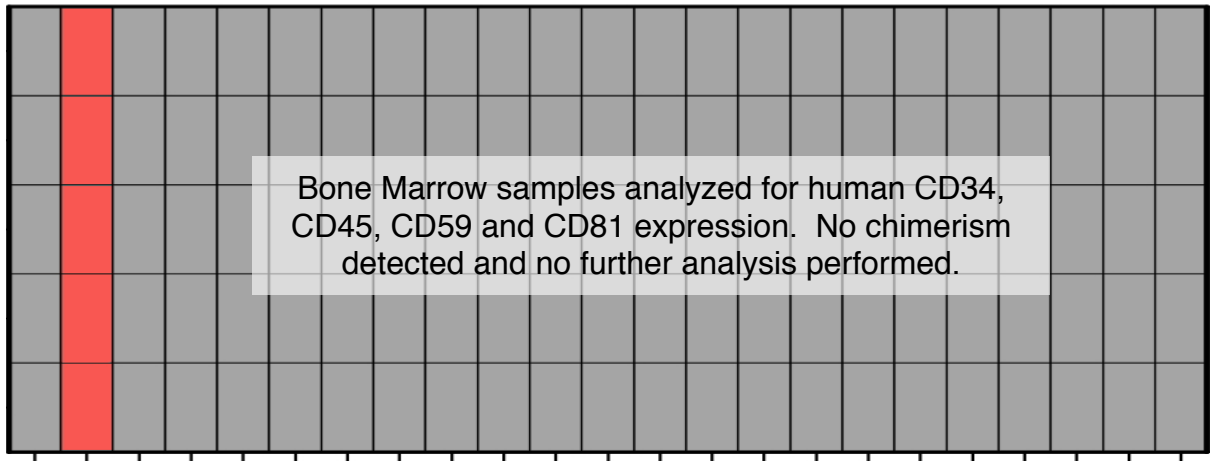


Age of Tissue

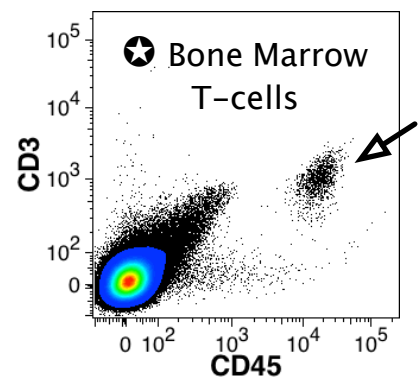
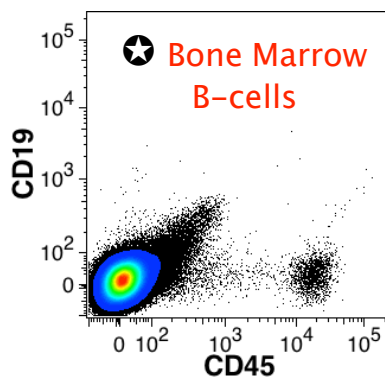
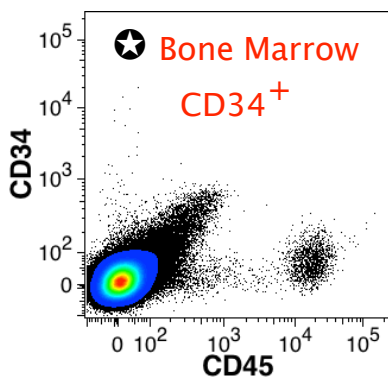
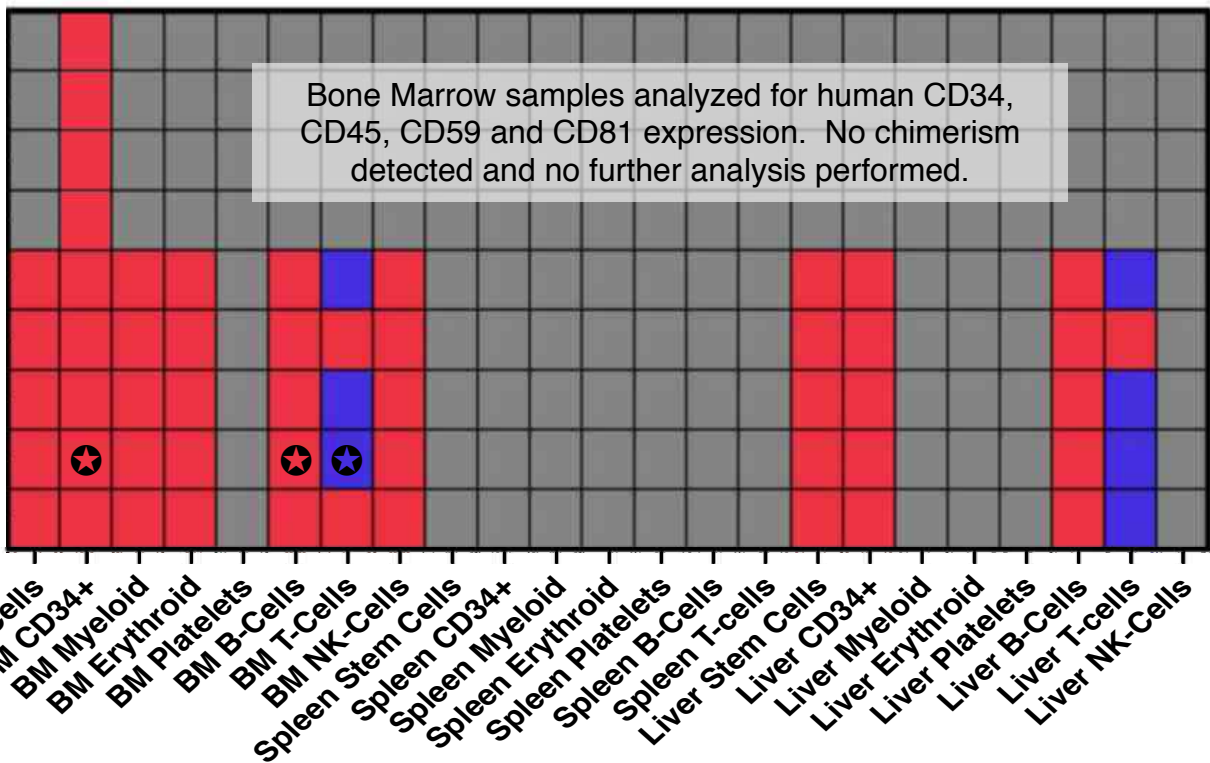
Engraftment



5.3 weeks



6.2 weeks



Tissue and Cell Population Analyzed

**Age of Tissue**

**Engraftment**

Not Determined No Engraftment Engraftment

**7.0 weeks**

Bone Marrow samples analyzed for human CD34, CD45, CD59 and  $\beta$ 2-microglobulin expression. No chimerism detected and no further analysis performed.

**8.5 weeks**

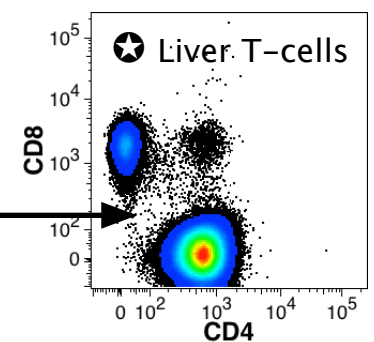
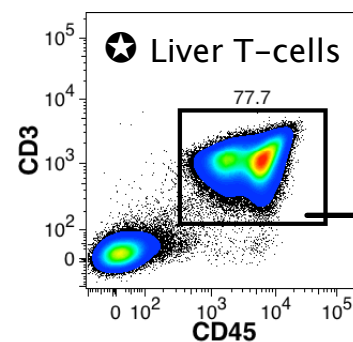
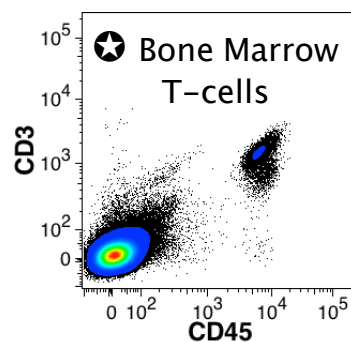
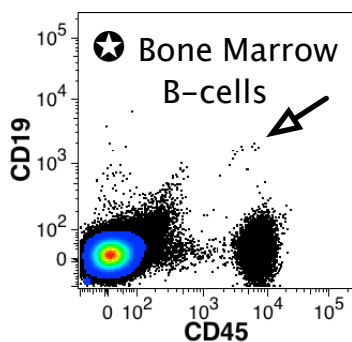
Bone Marrow samples analyzed for human CD34, CD45, CD59 and CD81 expression. No chimerism detected and no further analysis performed.

**10.3 weeks**

Bone Marrow samples analyzed for human CD34, CD45, CD59 and  $\beta$ 2-microglobulin expression. No chimerism detected and no further analysis performed.

**11.3 weeks**

BM Stem Cells  
BM CD34+  
BM Myeloid  
BM Erythroid  
BM Platelets  
BM B-Cells  
BM T-Cells  
BM NK-Cells  
Spleen Stem Cells  
Spleen CD34+  
Spleen Myeloid  
Spleen Erythroid  
Spleen Platelets  
Spleen B-Cells  
Spleen T-cells  
Liver Stem Cells  
Liver CD34+  
Liver Myeloid  
Liver Erythroid  
Liver Platelets  
Liver B-Cells  
Liver T-cells  
Liver NK-Cells



**Tissue and Cell Population Analyzed**

**Results for Individual Mice**

**Age of Tissue**

**Engraftment**

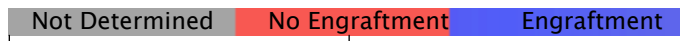


**Fig. S3**  
Page 3 of 11

**12.0 weeks**

Bone Marrow samples analyzed for human CD34, CD45, CD59 and  $\beta$ 2-microglobulin expression. No chimerism detected and no further analysis performed.

**13.0 weeks**

Bone Marrow samples analyzed for human CD34, CD45, CD59 and  $\beta$ 2-microglobulin expression. No chimerism detected and no further analysis performed.

**14.0 weeks**

Bone Marrow samples analyzed for human CD34, CD45, CD59 and  $\beta$ 2-microglobulin expression. No chimerism detected and no further analysis performed.

BM Stem Cells  
 BM CD34+  
 BM Myeloid  
 BM Erythroid  
 BM Platelets  
 BM B-Cells  
 BM T-Cells  
 BM NK-Cells  
 Spleen Stem Cells  
 Spleen CD34+  
 Spleen Myeloid  
 Spleen Erythroid  
 Spleen Platelets  
 Spleen B-Cells  
 Spleen T-cells  
 Liver Stem Cells  
 Liver CD34+  
 Liver Myeloid  
 Liver Erythroid  
 Liver Platelets  
 Liver B-Cells  
 Liver T-cells  
 Liver NK-Cells

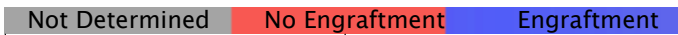
**Tissue and Cell Population Analyzed**

**Results for Individual Mice**

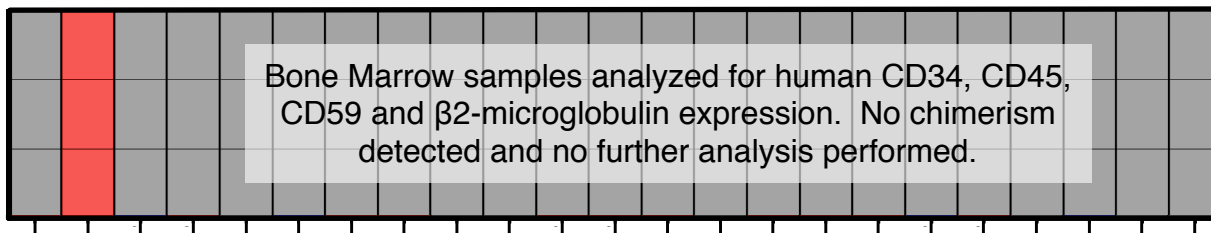


Age of Tissue

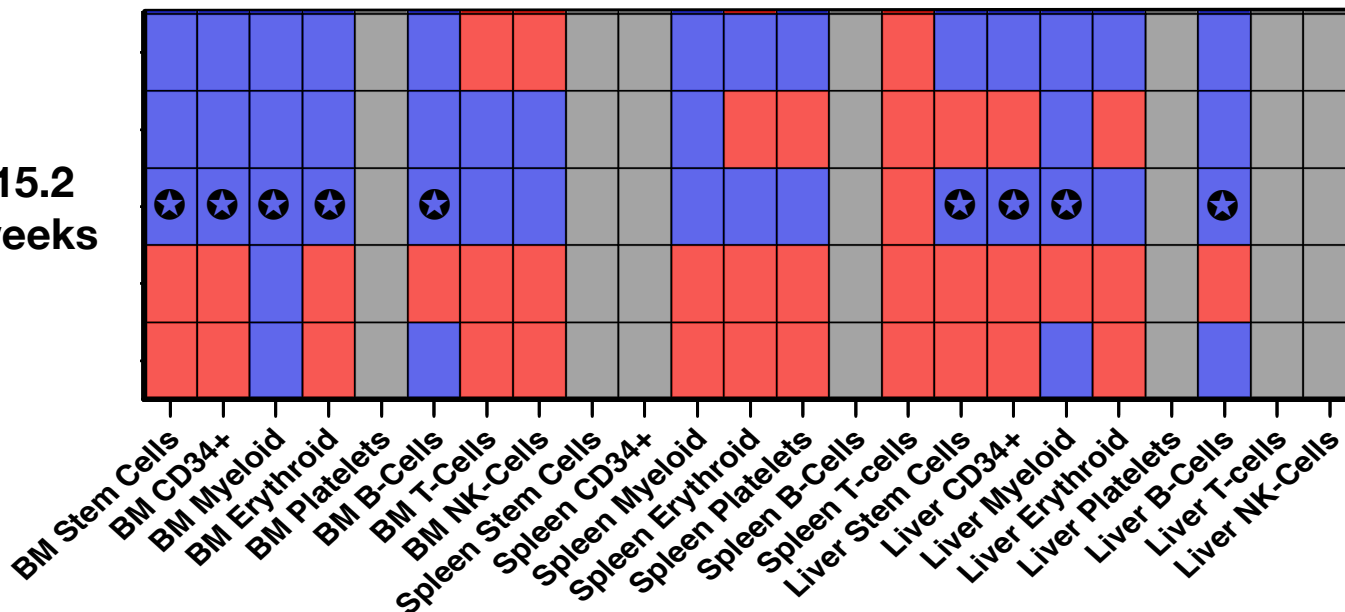
Engraftment



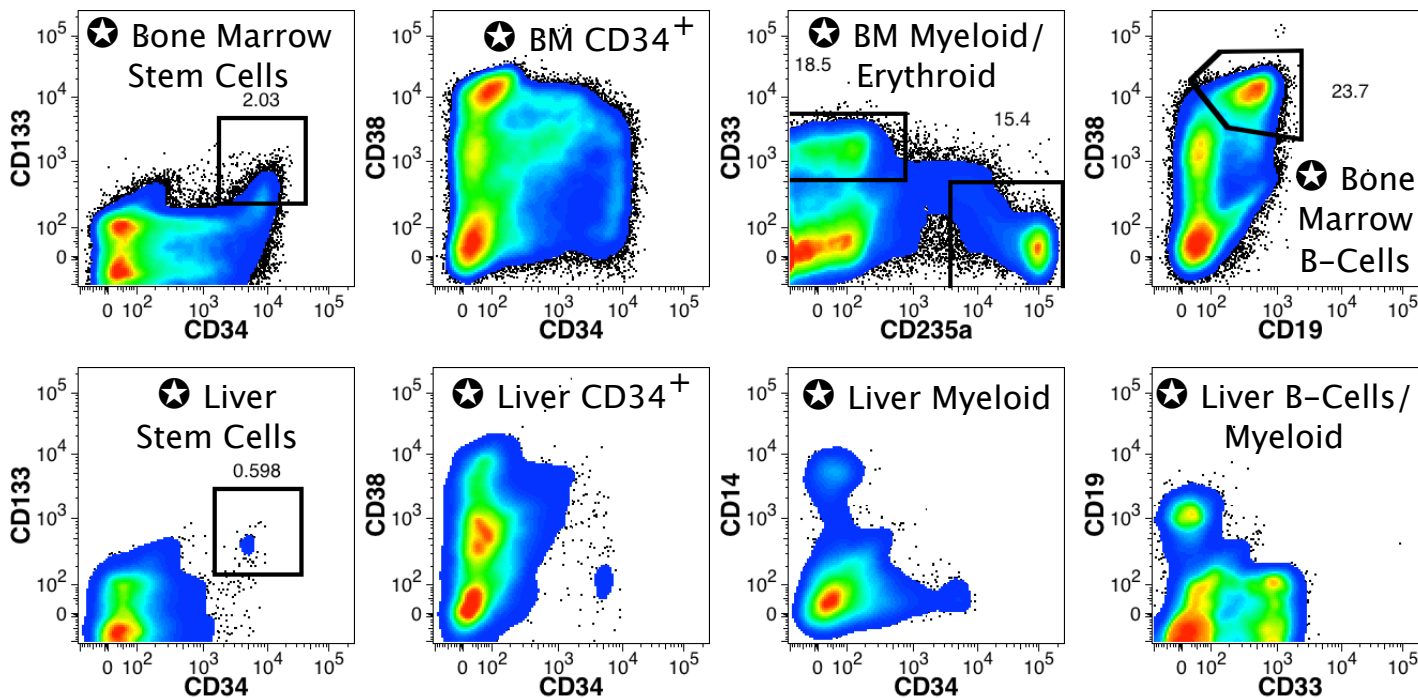
14.3 weeks



15.2 weeks



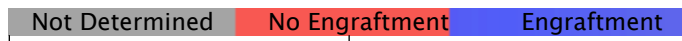
Results for Individual Mice



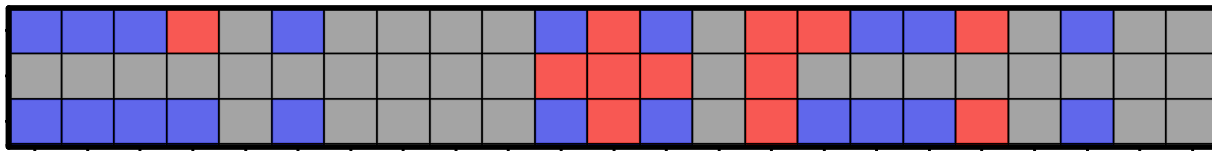
Tissue and Cell Population Analyzed

Age of Tissue

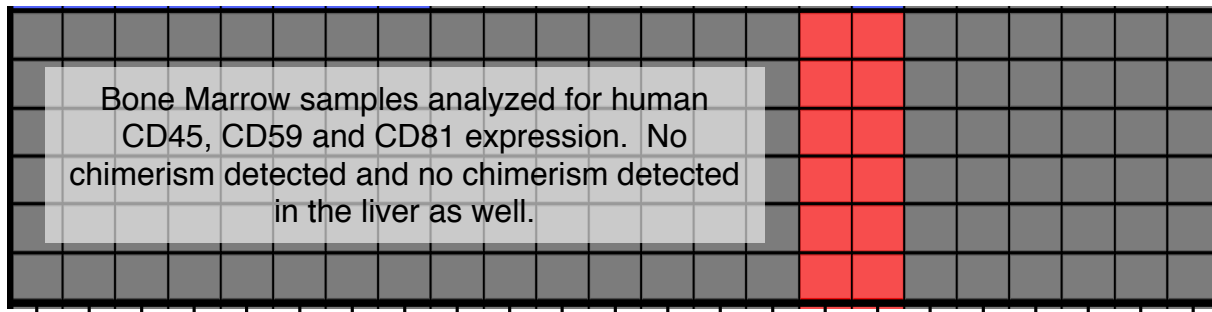
Engraftment



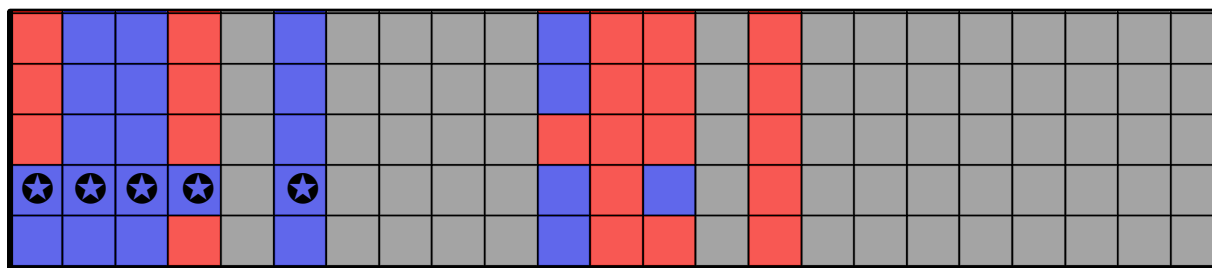
16.0 weeks



16.3 weeks

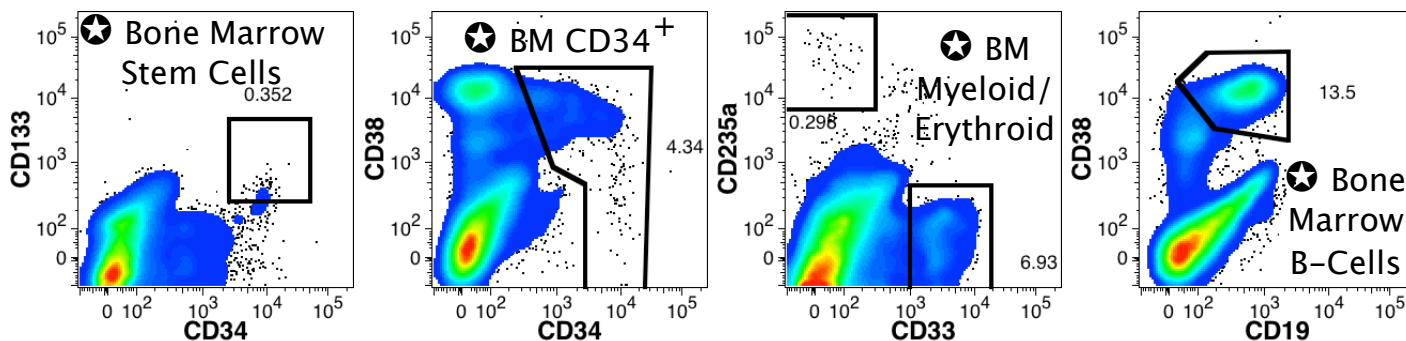


17.3 weeks



BM Stem Cells  
BM CD34+  
BM Myeloid  
BM Erythroid  
BM Platelets  
BM B-Cells  
BM T-Cells  
BM NK-Cells  
Spleen Stem Cells  
Spleen CD34+  
Spleen Myeloid  
Spleen Erythroid  
Spleen Platelets  
Spleen B-Cells  
Spleen T-cells  
Liver Stem Cells  
Liver CD34+  
Liver Myeloid  
Liver Erythroid  
Liver Platelets  
Liver B-Cells  
Liver T-cells  
Liver NK-Cells

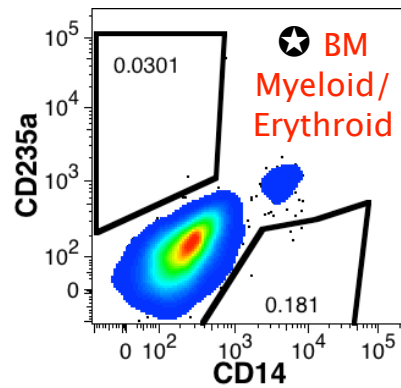
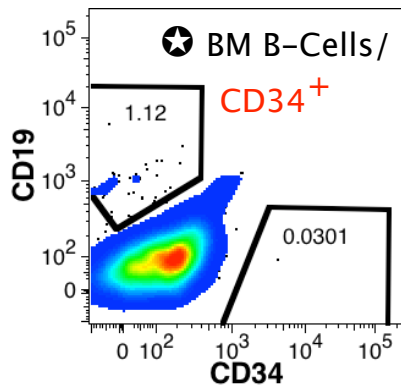
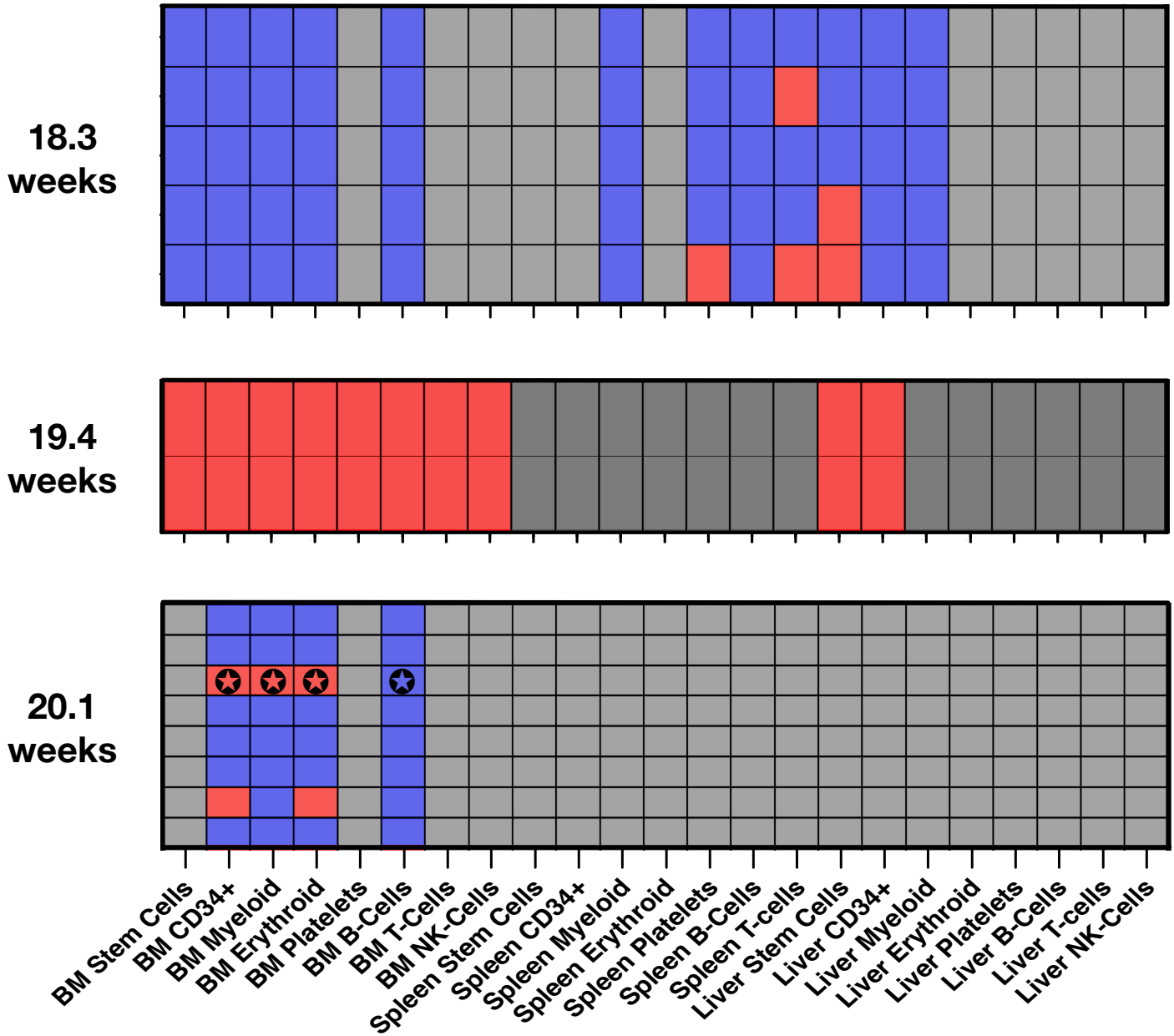
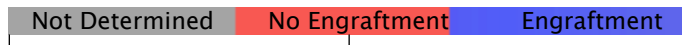
Results for Individual Mice



Tissue and Cell Population Analyzed

**Age of Tissue**

**Engraftment**



**Tissue and Cell Population Analyzed**



Age of Tissue

Engraftment

Fig. S3  
Page 7 of 11

Not Determined No Engraftment Engraftment

20.3 weeks

21.0 weeks

22.0 weeks

Fig. 6 Data →

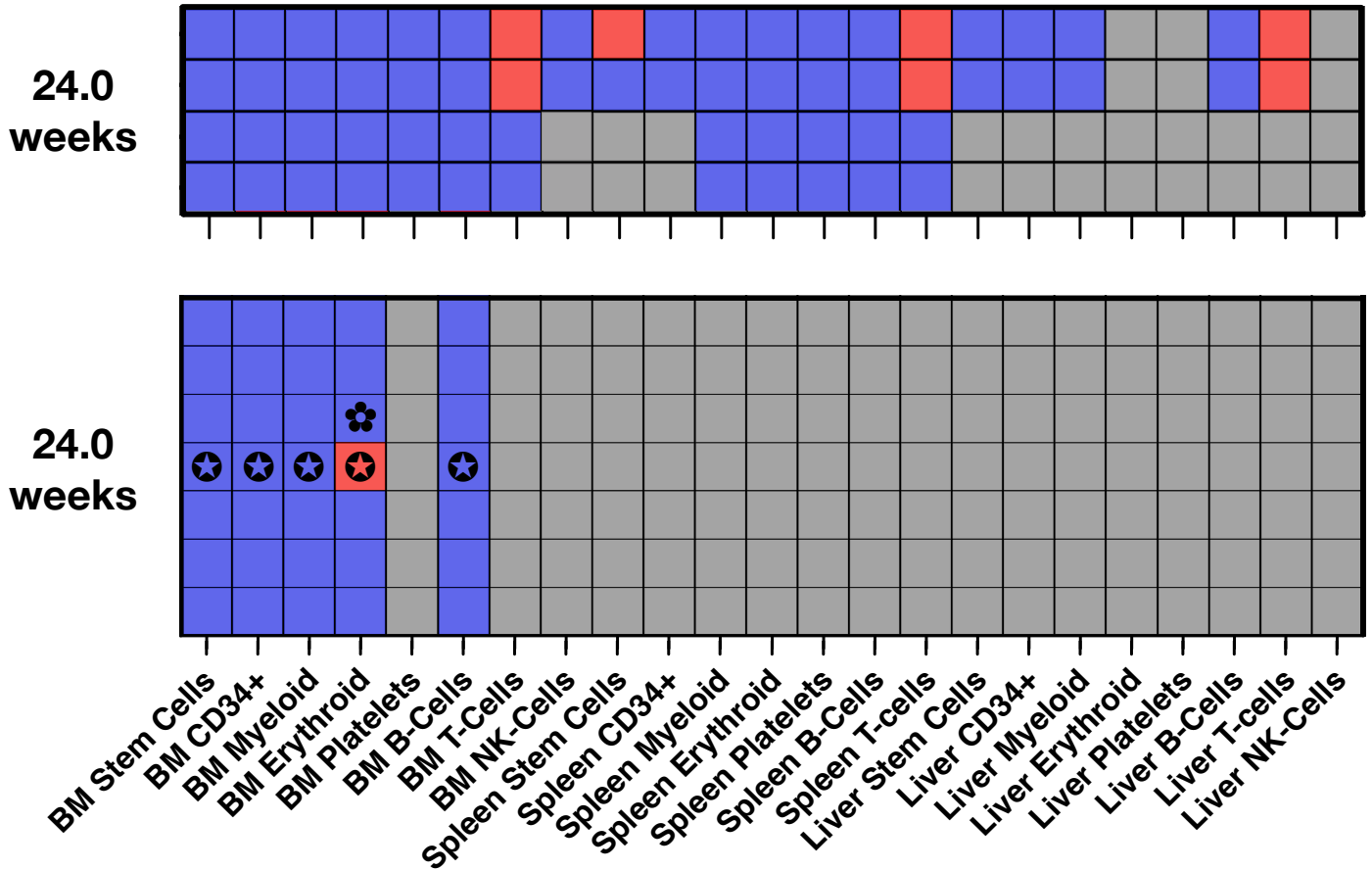
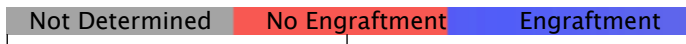
BM Stem Cells  
BM CD34+  
BM Myeloid  
BM Erythroid  
BM Platelets  
BM B-Cells  
BM T-Cells  
BM NK-Cells  
Spleen Stem Cells  
Spleen CD34+  
Spleen Myeloid  
Spleen Erythroid  
Spleen Platelets  
Spleen B-Cells  
Spleen T-cells  
Liver Stem Cells  
Liver CD34+  
Liver Myeloid  
Liver Erythroid  
Liver Platelets  
Liver B-Cells  
Liver T-cells  
Liver NK-Cells

Tissue and Cell Population Analyzed

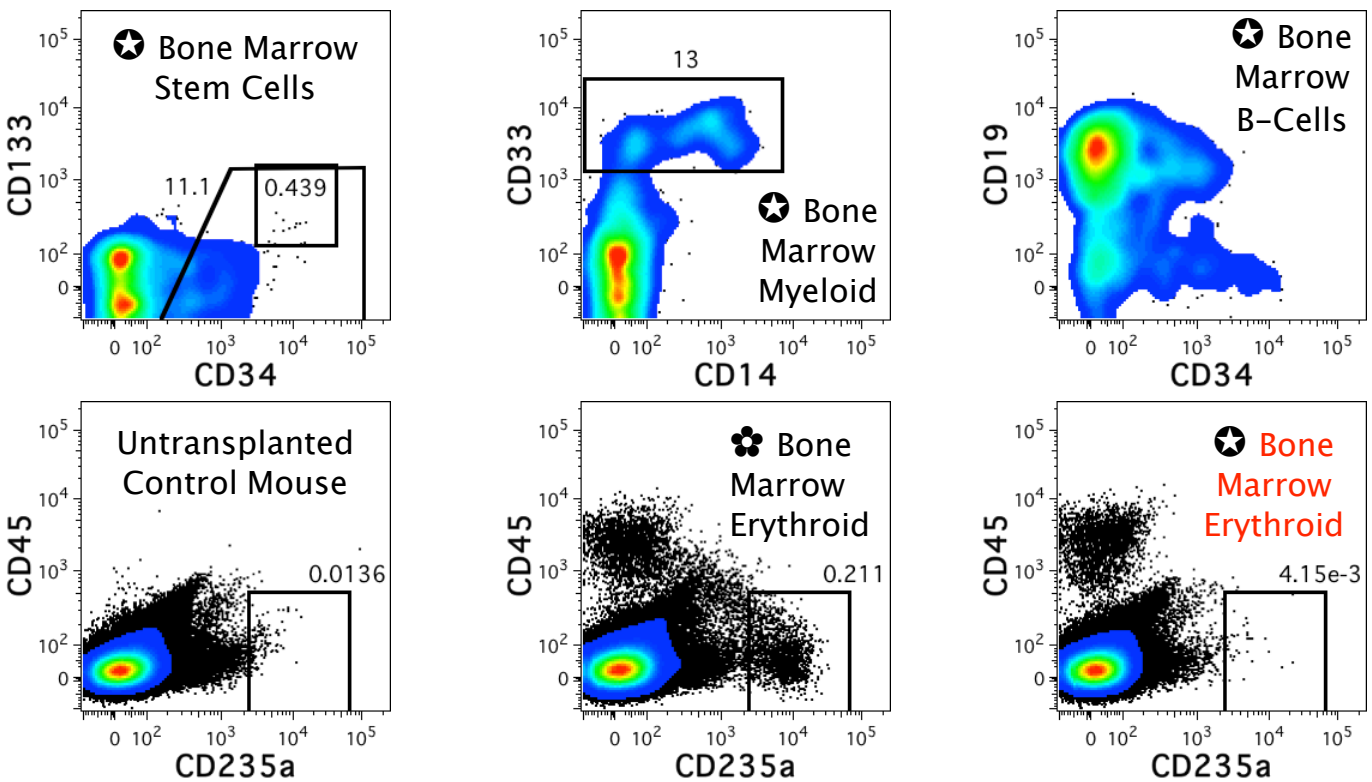
Results for Individual Mice

Age of Tissue

Engraftment



Results for Individual Mice

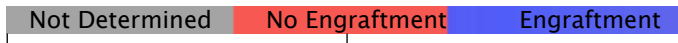


Tissue and Cell Population Analyzed

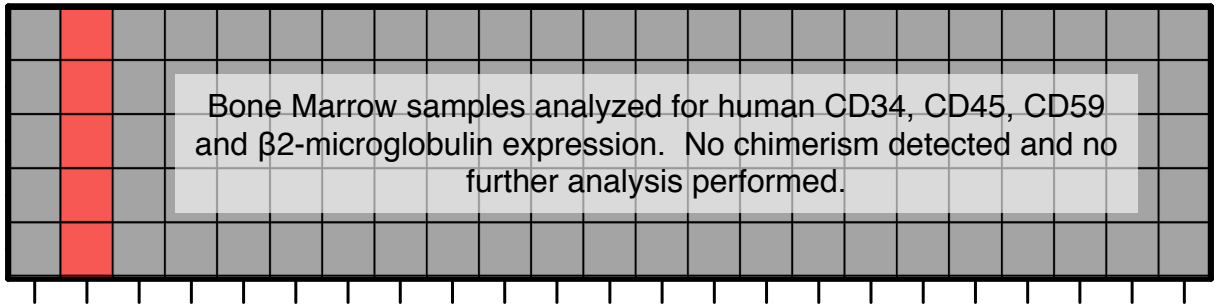
Age of Tissue

Engraftment

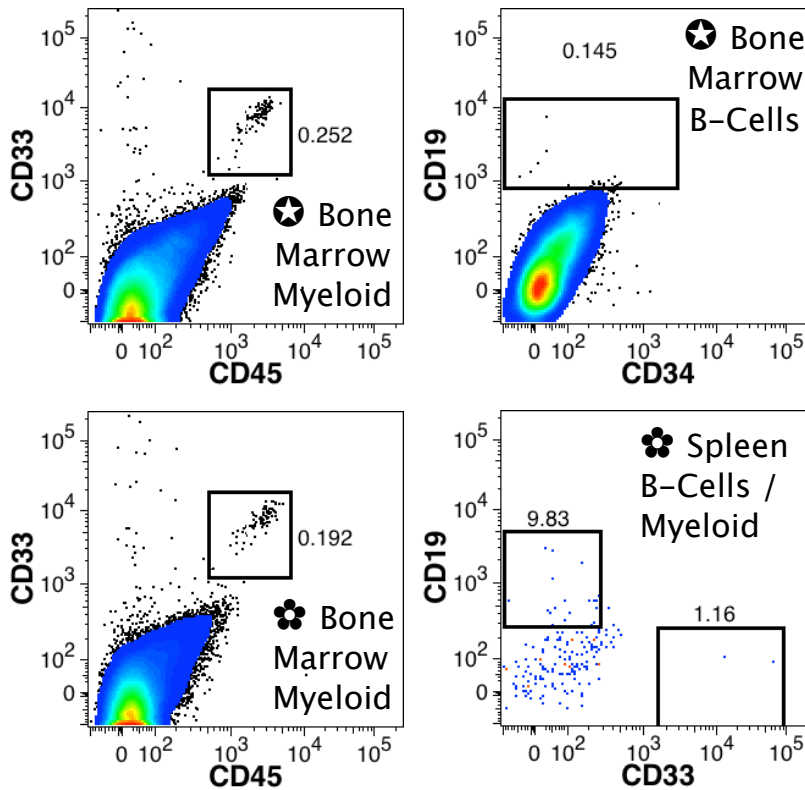
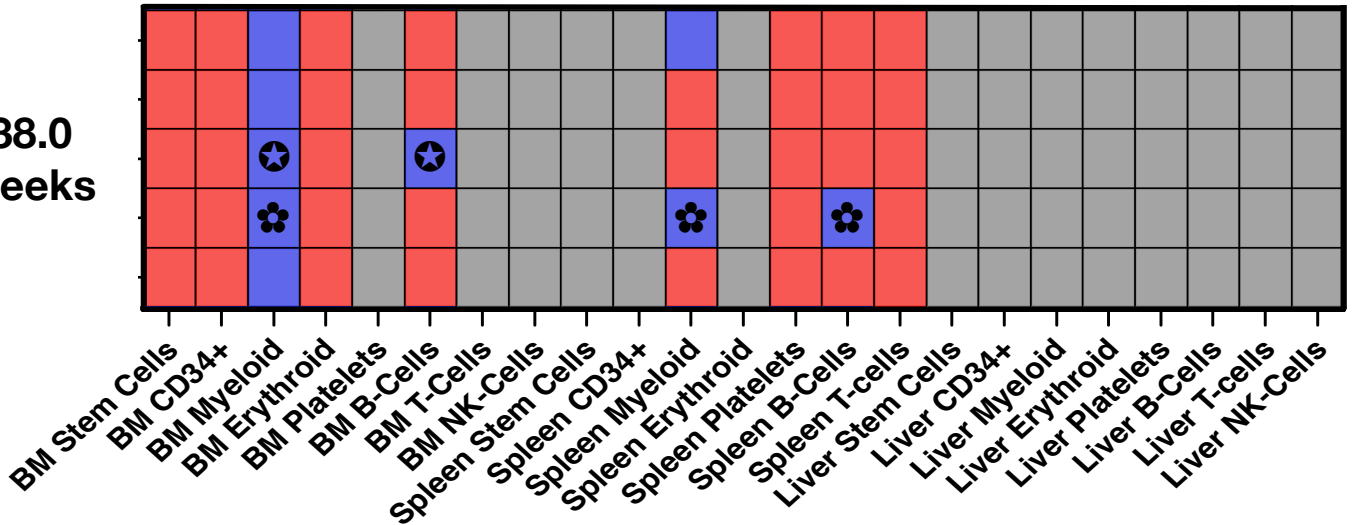
Fig. S3  
Page 9 of 11



34.5 weeks



38.0 weeks



Tissue and Cell Population Analyzed

Results for Individual Mice



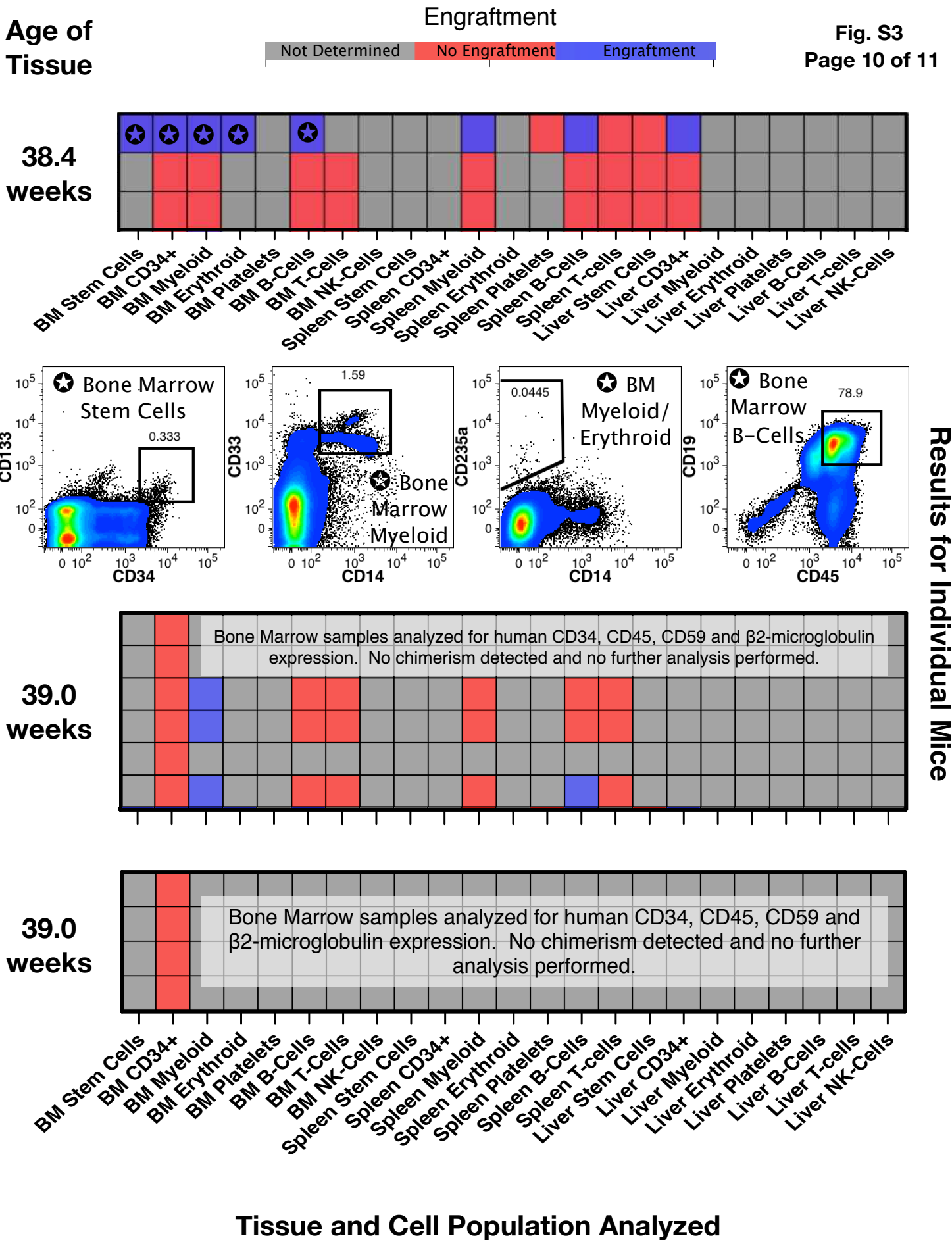
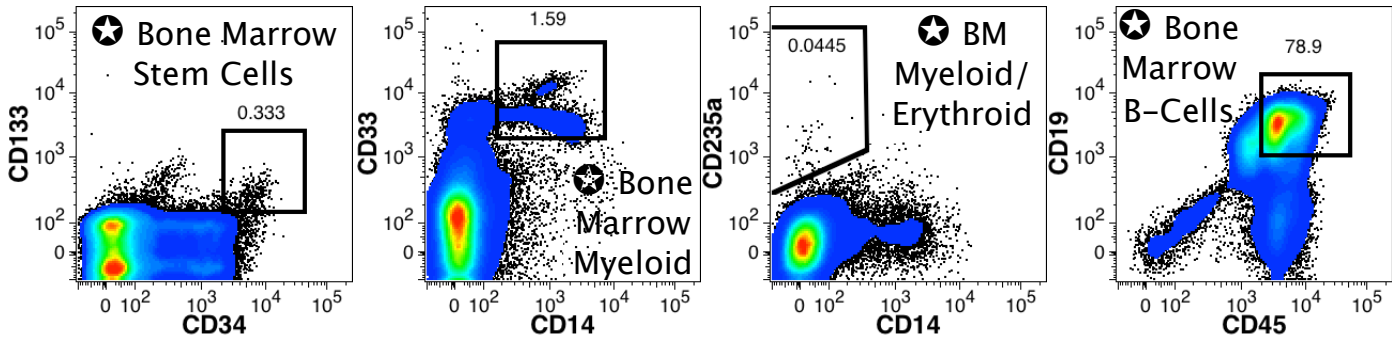


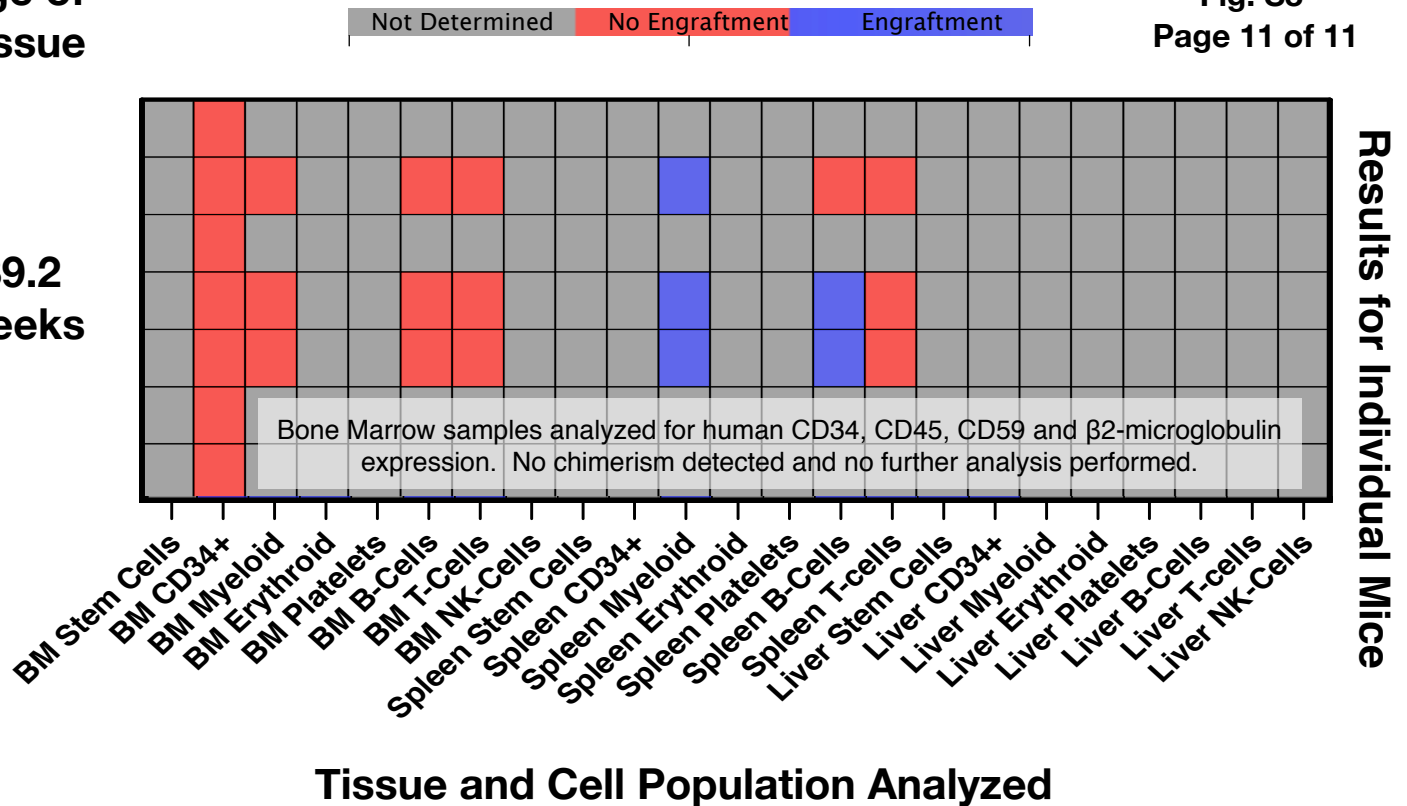
**Fig. S3**  
Page 10 of 11

**Results for Individual Mice**

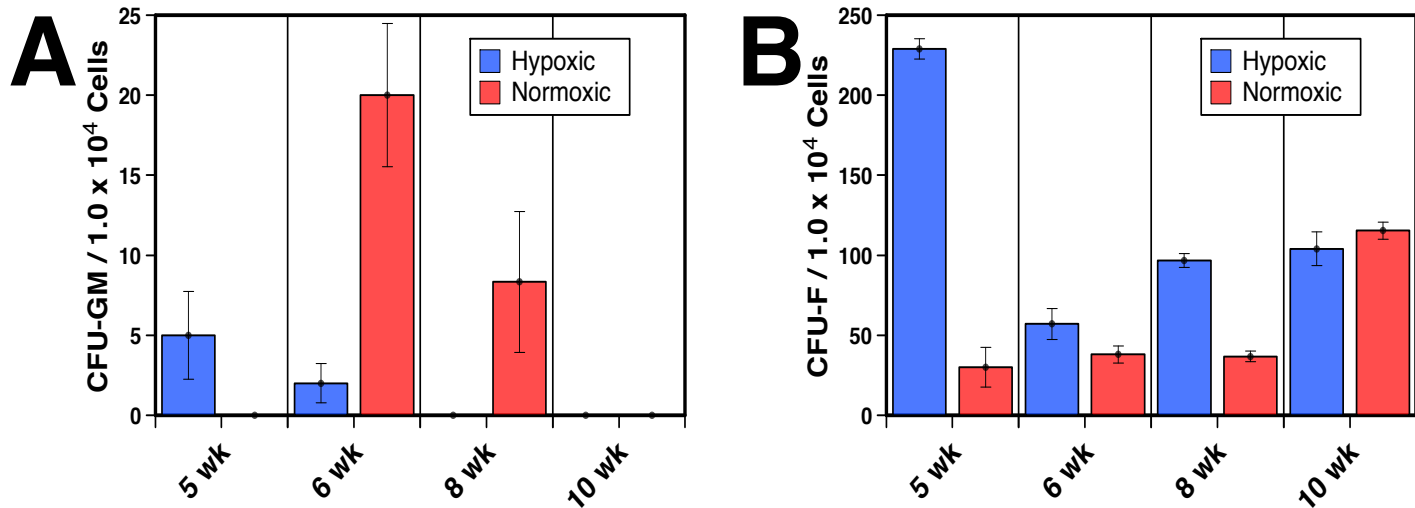


Age of  
Tissue

## Engraftment

Fig. S3  
Page 11 of 1139.2  
weeks

**Fig. S3. Overview of hematopoietic engraftment and selected flow cytometric analyses of chorion transplants in immunodeficient mice.** Heat maps indicate the lineage analyses performed for the three hematopoietic tissues examined and whether engraftment was observed for each of the 28 transplanted cell isolates. Results are presented according to gestation age of the donor tissue (youngest at the top), which parallels the presentation of the summary findings presented in Fig. 5B of the manuscript. Each row of a heat map represents a single transplanted mouse. At a minimum, all mice were analyzed with a single panel of antibodies staining widely expressed human antigens (CD34, CD45, CD59 and CD81 or  $\beta$ 2-microglobulin). If no human chimerism was detected, then no further analysis was performed. Otherwise, mice were analyzed for the presence of human CD34+, myeloid, erythroid and B-lymphoid bone marrow cells in addition to any other indicated tissue/lineage analyses. Fig. 6 in the manuscript presents a broad analysis of hematopoietic engraftment in one mouse. Additional examples of flow cytometry results showing full and partial engraftment are presented herein: 1) First trimester tissues generally did not engraft mice with the exception of T- and B-lymphocyte engraftment observed in some mice (6.2 and 11.3 weeks' gestation grafts), 2) the youngest tissue yielding full engraftment was 15.2 weeks' gestation, 3) another examples of full engraftment is shown for the 17.3 weeks' gestation graft, 4) an example of partial (B-cell) engraftment is shown for the 20.1 weeks' gestation sample, 5) another example of partial engraftment in which erythroid engraftment could not be documented is shown for one of the 24.0 weeks' gestation samples, 6) partial myeloid engraftment was observed in some transplants of third trimester tissues - e.g, 38.0 weeks' gestation- with very low numbers of CD19+ cells being observed as well, in some cases, and 7) a single case of full engraftment was observed in a mouse transplanted with third trimester cells (38.4 weeks' gestation). The symbols  $\odot$  and  $\oplus$  are used to indicate the mouse, tissue and cell lineage represented by the flow cytometry data shown associated with the individual heat maps. Analyses labeled with red text represent negative data and black text represents positive engraftment data.



**Supplemental Figure S4. Oxygen levels do not significantly affect the in vitro hematopoietic potential of 1<sup>st</sup> trimester chorionic hematopoietic progenitors.** Prior to 7 wks the chorion and the chorionic villi could not be separated and were analyzed together. Afterwards the chorion was processed separately from the villi. Cells were cultured for 3 wks in either physiological hypoxia (1% O<sub>2</sub>, blue) or standard conditions (20% O<sub>2</sub>, red). (A) CFU-GM (granulocyte-macrophage) colonies were enumerated at the gestational ages indicated. (B) CFU-F (fibroblast) colonies in the same cultures were also enumerated. Data in A and B are mean ± SEM of 3-5 plates/sample.

Supplementary Table S1. This table contains a full list of the monoclonal antibodies against human and mouse antigens utilized in flow cytometry analyses, including the fluorochrome label, isotype, clone name and source.

[Click here to Download Table S1](#)